2015

Injectable Conductive Hydrogels for Use in Neuroprosthetic Intervention

Rosa Ghatee
University of Rhode Island, rosa_ghatee@uri.edu

INJECTABLE CONDUCTIVE HYDROGELS FOR USE IN NEUROPROSTHETIC INTERVENTION

BY

ROSA GHATEE

A THESIS SUBMITTED IN PARTIAL FULFILLMENT OF THE REQUIREMENTS FOR DEGREE OF

MASTER OF SCIENCE

IN

ELECTRICAL ENGINEERING

UNIVERSITY OF RHODE ISALND

2015

MASTER OF SCIENCE THESIS

OF

Rosa Ghatee

APPROVED:

Thesis Committee:

Major Professor Stephen M. Kennedy

Samantha A. Meenach

Walter G. Besio

Nasser H. Zawia
DEAN OF THE GRADUATE SCHOOL

UNIVERSITY OF RHODE ISLAND
2015

Abstract

Neuroprosthetic interventions are strategies aimed at treating a wide range of neurological disorders, long-term neuroprosthetic treatments traditionally require the implantation of hard metallic electrodes that must sustain their electrical connection with neural tissues for prolonged periods of time. However, surgical introduction of these electrodes and their mechanical mismatch with neural tissues results in inflammation, which disrupts their electrical interface. Our aim was to develop soft, injectable, and conducting hydrogel-based electrode materials and characterize their sustained mechanical and electrical properties before and after sterilization and injection. These gels were made from poly (3-4, ethylenedioxythiophene) (PEDOT) (a conductive polymer) and poly (acrylic acid) (PAAc) and were polymerized at subfreezing temperatures to generate soft 3D macroporous structures. These porous hydrogels exhibited enhances mechanical properties. When optimized, gels exhibited softness consistent with neural tissues (<100 kPa), excellent toughness (>2 kJ/m^3), and excellent strain-at-failure (survived >90% compression without failure). Additionally, these gels' mechanical properties could be tuned by altering their compositions, though their conductivity remained almost constant and independent of gels composition at about 1 S/cm. This conductivity was much higher than neural tissues making them well-suited for stimulating the sensing in neuroprosthetic applications. Finally, because of their optimized mechanical properties, these gels were highly compressible, exhibited further enhanced electrical properties when compressed, and were capable of surviving injection through 16-gauge needles.

Acknowledgements

I would like to express my sincere gratitude to my advisor Dr. Stephen Kennedy for his continuous advice and support of my master study and related research, for his patience, motivation, and immense knowledge. His guidance helped me during the research and writing of this thesis. I could not have imagined having a better advisor and mentor.

Besides my advisor, I would like to thank the rest of my thesis committee: Dr. Samantha Meenach and Dr. Walter Besio, for their support. Dr. Meenach and Dr. Besio granted me access to instruments and equipment needed for my research and I would not have been able complete this work without their assistance and support. I also want to Thank Dr. Everett Crisman for his suggestions and help with SEM imaging. I would also like to thank Anita Tolouei for her help with SEM imaging.

I'd like to thank my fellow labmates in for the stimulating discussions, for the sleepless nights we were working together before deadlines, and for all the fun we have had in the last year.

Last but not the least, I would like to thank my family: my parents and to my sisters for supporting me spiritually throughout writing this thesis and my through my life.

Funding for this work was supported through start-up funds from the University of Rhode Island's College of Engineering (Kennedy), an Early Career

Development Award from the RI-INBRE (NIH/NIBMS 2P20GM103430 and an NSF EPSCoR grant (1539068).

Preface

This thesis has been presented in manuscript format according to guidelines of the graduate school of the University of Rhode Island. The complete thesis represents one manuscript. The first and only manuscript (Chapter 1) is prepared for submission to *Biomaterials* with authors R. Ghatee, W. Besio, and S. Kennedy.

Table of Contents

List of Figures

Chapter 1

Prepared for submission to *Biomaterials*

Injectable Conducting Hydrogels for Use in Neuroprosthetic interventions

Rosa Ghatee, Walter G. Besio, Stephen M. Kennedy

Department of Electrical, Computer and Biomedical Engineering, University of Rhode Island, Kingston, RI, USA

Corresponding Author:

Stephen M. Kennedy

Department of Electrical, Computer and Biomedical Engineering and Chemical Engineering

University of Rhode Island

Kingston, Rhode Island, 02881, USA

skennedy@ele.uri.edu

1. Introduction

Up to one billion people worldwide are affected by neurological disorders (e.g. Alzheimer's, Parkinson disease, and epilepsy). This number is estimated to increase considerably (Fig. 1A), particularly due to the rise of life expectancy. The degree to which people are debilitated by these neurological problems rivals and exceeds some of the worst ailments in existence (e.g. HIV, heart disease, and cancer) (Fig. 1B) (World Health Organization, 2006). Neuroprosthetic devices are developed in order to return the function or to reduce the symptoms exhibited by patients suffering from neurological diseases (Leache et al.). For instance, electrical therapies such as auditory implantation (Zeng et al., Wilson et al.), deep brain stimulation (Williams et al., Lyons), spinal cord functional electrical stimulation (FES) (Carmel et al., Minassian et al.), spinal cord stimulation (SCS) (Tilley et al.), and vision prosthesis (Fridman et al., Pezaris et al) are promising strategies in treating patients with severe neurological diseases. While promising, these strategies are not without limitations (Leach et al.). These strategies require a stable electrode-tissue interface which does not vary over time (Hassarati et al.). Electrodes must: (i) minimize the overpotential at the tissue-electrode interface and (ii) maintain an electrically conductive path between the electrode and the tissue being stimulated.

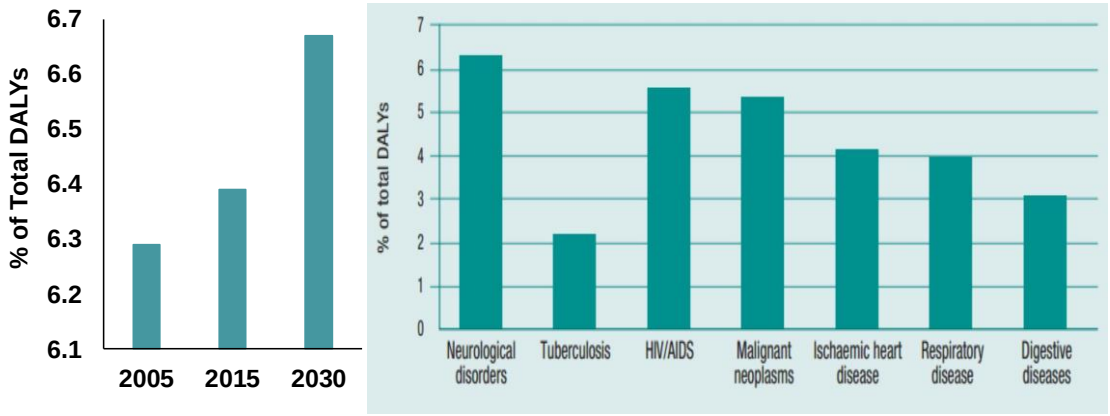

Figure 1. Neurological diseases and disorders are affecting people at an increasing rate and are more disabling than many other problematic diseases. **A**. The percentage of global Disability-Adjusted Life Year (DALYs) for 2005 and projected for 2015 and 2030 in order to highlight the increasing burden constituted by neurological disorders. Part A adapted from World Health Organization; Neurological disorders public health challenges; 2007. **B**. The percentage of global DALYs for 2005 in order to highlight the burden constituted by neurological disorders compared to other common diseases. Part B is from World Health Organization; Neurological disorders public health challenges; 2007.

Traditionally, metallic electrodes are used in these situations and have outstanding electrical properties over a short period of time. However, they do not maintain these properties over protracted periods of time (Green et al. (2008), Leach et al., Rousche et al.), which is of particular importance for treating neurological disorders that require long-term intervention (e.g. deafness, blindness, epilepsy, Parkinson's Disease, etc.). Implanting these electrodes into neural tissue (Fig. 2A) results in an initial period of electrical conductivity; however, this conductivity is thought to be lost over time for number of reasons. First, electrode introduction requires invasive surgery (Zeng et al., Wilson et al) which results in blood vessel and neuron rupture. This traumatic electrode introduction results in an initial degree of conductivity, but starts the foreign body response (Fig 2B) (Leach et al.). Later on, loss of conductivity is likely due to the micromotion (Rousche et al., Leach et al.) which results from a mismatch in stiffness between the electrodes and the tissue. This mismatch causes shear stress at the interface, resulting in inflammation, glial tissue development (Fig. 2C), increased

electrical impedance, and eventually, decreased electrical connection (Fig 2D) (Asplund et al., Green et al. (2012), Rousche et al.). Thus, conductive materials are needed that are injectable and soft in order to reduce inflammation and to maintain electrical connectivity with neural tissues for longer periods of time. In this study, we therefore aimed to develop a novel hydrogel-based electrode whose mechanical properties mimic those of native tissue and that can be introduced through a minimally invasive injection.

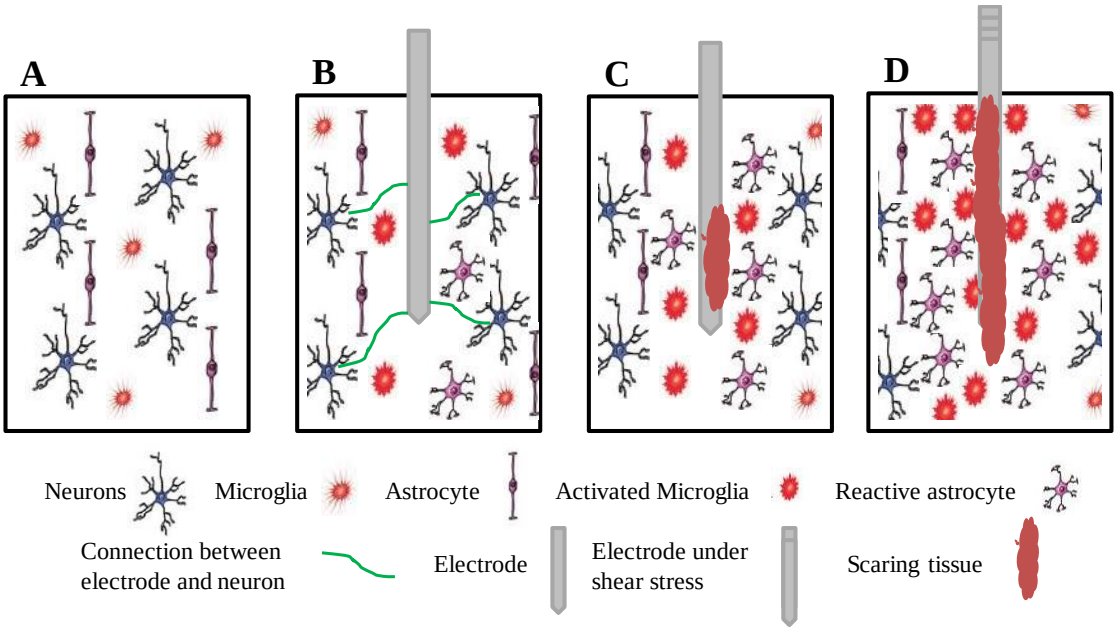

Figure 2: **After implantation, metal electrodes lose their conductive connection to neurons over time. A**. Normal neural tissue before electrode insertion (tissue is not in an inflamed state). That is, microglia is inactivated and astrocytes are not in a reactive state. **B**. After the insertion of the electrode inflammation begins, but neurons and the electrode are still in contact with neurons. **C**. As time goes on, this inflammation results in scare tissues, which isolates the electrodes from the neurons. Activated microglia and reactive astrocytes start blocking the electrode and from neurons **D**. Chronic inflammation due to mismatch between brain tissue and electrode will result shear stress and causes more migration and attachment of scarring and glial tissue at the surface of the electrode. This further isolates prevents electrical connectivity between the electrode and the neurons.

In order to help reduce inflammation and the associated loss in conductivity when implanted for prolonged periods of time, electrodes developed here were designed to have tissue-like mechanical properties by virtue of being made in a hydrogel format. Hydrogels are soft materials which are made from cross-linked hydrophilic polymer

networks (Pan et al.), that have the potential to be loaded with and locally deliver therapeutic agents such as anti-inflammatories (Kearney and Mooney). Unlike traditional electrode materials, hydrogels have similar mechanical properties as physiological tissues, which make them useful in a wide variety of biomedical applications (Dee et al.). However, they normally have poor conductivity (Saracino et al.). Although poor conductivity is not an issue in many applications, for use as electrodes in neuroprosthetic interventions, conductivity is a critical priority (Cheong et al.; Leach et al.). Conductive polymer hydrogels are a unique class of hydrogels that not only have similar mechanical properties as neural tissue (Aregueta-Rables et al.), but also have electrical properties similar to metals and inorganic semiconductors (Zhao et al.). It has recently been demonstrated that hydrogels composed of Poly (3-4, ethylenedioxythiophene) (PEDOT) provide electrical conductivity (Fig. 3A) and stability in oxidized environments (Cheong et al.; Abidian et al. (2006); Abidian et al. (2008); Huange et al.; Naficy et al.; Sekine et al.). Moreover, PEDOT hydrogels are biocompatible (Cho et al.) and can have similar Young's moduli as neural tissues (Fig. 3B). For these reasons, PEDOT was employed as the conductive component of the hydrogel-based electrodes described here.

A

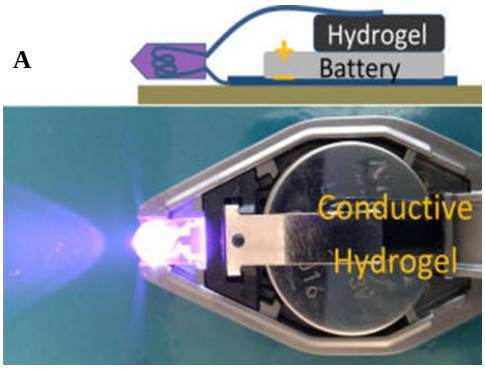

C

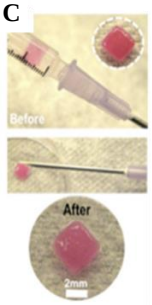

B

Material	Young's Modulus (KPa)
Hydrogel (PAA) (Gulyuz et al.)	183-605
PAA-PEDOT (estimated from Naficy et al.)	100
Neural Tissue (Leach et al.)	~100

Figure 3. PEDOT hydrogels can be made to be electrically conductive and soft like neural tissues. **A**. Demonstration of PEDOT hydrogel conductivity showing that it can be used to complete an LED circuit (Naficy et al.). **B**. A table comparing the Young's moduli of a traditional hydrogels (poly acrylic acid) with conducting hydrogels (PEDOT) and neural tissues. **C**. Images showing that a gel retains its shape after injection **(**Bencherif, et. al**)**

Finally, to further minimize inflammation, these hydrogel-based electrodes were designed to be injectable by being endowed with shape-memory properties. Shape memory polymers are a class of polymers which can change their shape temporarily due to the change in the temperature, pressure, or pH and regain its original shape (Pilate et al.). This property allows for minimally invasive implantation (Wang et al.). These hydrogel-based electrodes were fabricated using a cryogelation approach, which results in hydrogel structures with interconnected macropores (Kumar and Sirvastava). The sponge-like "cryogels" are capable of being injected by being passed through a standard 16-gauge needle (Fig. 3C, top). The cryogels retain their structural integrity after injection (Fig. 3C, bottom). Additionally, the cryogelated hydrogels have moduli (Kennedy et al.) similar to tissue (i.e., 10s-100s kPa) (Engler et al.), and have sufficient

mechanical toughness to remain intact and mechanically consistent when exposed to cyclic compression (50% compression, 1000 cycles) (Cezar et al.).

We hypothesized that PEGDM-cross-linked poly(AAc) gels that encapsulate PEDOT polymers will exhibit softness, toughness, compressibility, be injectable, while also being electrically conductive. Our goal in this study was to create an injectable conductive hydrogel which we were expected to be extremely tough comparing to other hydrogels. Our approach involves the use of a PEGDM-cross-linked anionic poly(AAc) hydrogel network to entrap cationic PEDOT polymer. Beyond the covalent PEGDM cross-links holding the gel together (which are highly bio-compatible), these polymer choices provide a high density of electrostatic interactions between negatively charge poly(AAc) and positively charged PEDOT (i.e., ionic cross-links). These electrostatic interactions are broken, absorbing energy when the gel is compressed. However, after breaking and absorbing energy, these broken ionic cross-links can re-cross-link with other positive/negative charges in the network, as they are bountiful in interpenetrating poly(AAc)/PEDOT networks. We believe this strategy will produce gels with the enhanced toughness required for injectability and for long-term survival after injection, while retaining the electrical conductivity of PEDOT and while still maintaining the softness of a hydrogel material.

2. Materials and Methods

2.1 Materials

Acrylic acid (AAc), Sodium hydroxide (NaOH), Poly (ethylene glycol) dimethacrylate (PEGDM), Poly (3-4, ethylenedioxythiophene): polystyrene sulfunate (PEDOT:PSS), N,N,N',N'-Tetramethylethylenediamine (TEMED), ammonium Persulfate (APS), and Phosphate buffered saline (PBS) were purchased from Sigma Alrdrich. Except Acrylic acid, the rest of materials were used without any changes. Acrylic acid was purified with aluminum oxide column to remove inhibitor.

2.2 Gel fabrication

To make non-macroporous gels, gels were fabricated at room temperature (RT). Different amounts of AAc (4 wt % to 10 wt %), PEGDM (1, 2, and 5 wt %), NaOH (465 µg per ml of AAc), deionized water (DI water), and PEDOT:PSS (2.6 wt %) were mixed by vortexing. Then TEMED (58.2 mg per ml of solution) and APS (3.4 mg per ml of solution) were added to initiate gelation (Fig. 4A). The solutions were immediately transferred to a 10 x 10 mm cylindrical Teflon molds and left to gel at room temperature for about three hours in order to form a PEGDM-cross-linked poly(AAc) network that physically entrapped PEDOT (Fig. 4B). Gels were soaked in PBS three days prior to running tests. To make gels with enhanced mechanical properties for softness and injectability, macroporous gels were made as described above, however, they were cryogelated in 10 x 10 mm cylindrical Teflon molds at -20˚C and left to gel at -20 ˚C overnight. This results in a concentrated PEGDM-cross-linked poly(AAc) network with entrapped PEDOT that exists between ice crystals. When the ice crystals

are thawed, the result in a macro-porous structure with a concentration PEGDM-cross-linked network with entrapped PEDOT existing between macro-pores (Fig 4C).

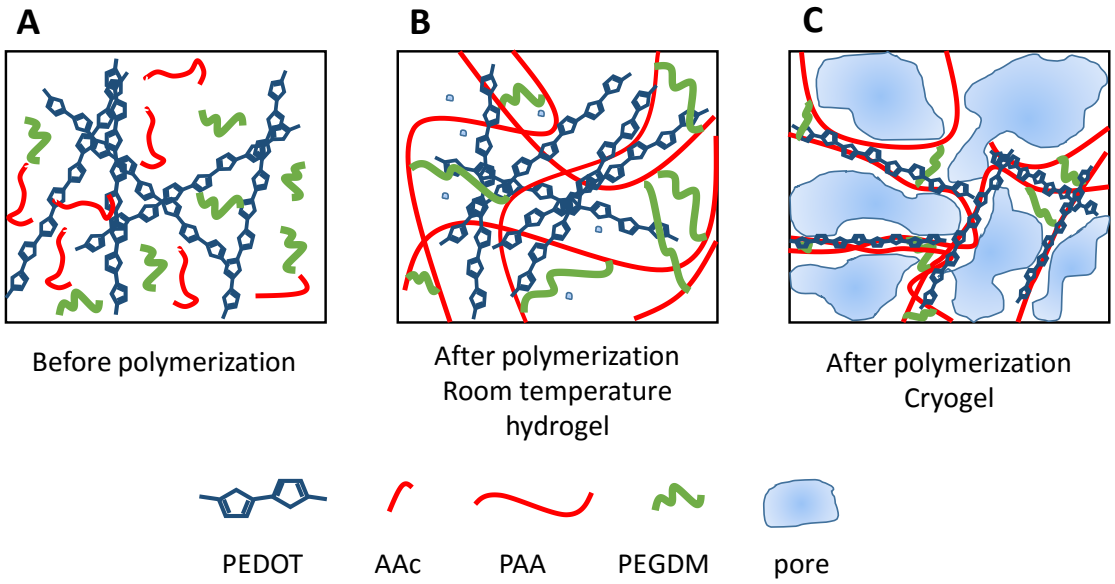

Figure 4: The fabrication process of porous cryogels endow them with higher concentration of PAA-PEGDM-PEDOT between pores as compared to gels made at room temperature. **A**. Schematic of mixture before polymerization starts. **B**. Schematic of room temperature hydrogel after gelation. **C**. Schematic of cryogels after cryogelation.

2.3. Gel mechanical and structural characterizations

Gel stiffness (modulus), strain at failure, and toughness were quantitatively measured using a compression test. Gels of various compositions were placed between the plates of an Instron (Model 3345) and compressed until they structurally failed (Fig. 5A). After running the compression test on a given gel, a stress-strain curve (Fig. 5B, blue curve) was obtained. Several critical mechanical parameters (i.e., Young's modulus, ultimate tensile strength, strain of failure, and toughness) were extracted from these stress-strain curves (Fig. 5B, red, purple, green dashed lines and area under the curve, respectively). For detailed calculation please see appendix A.1.

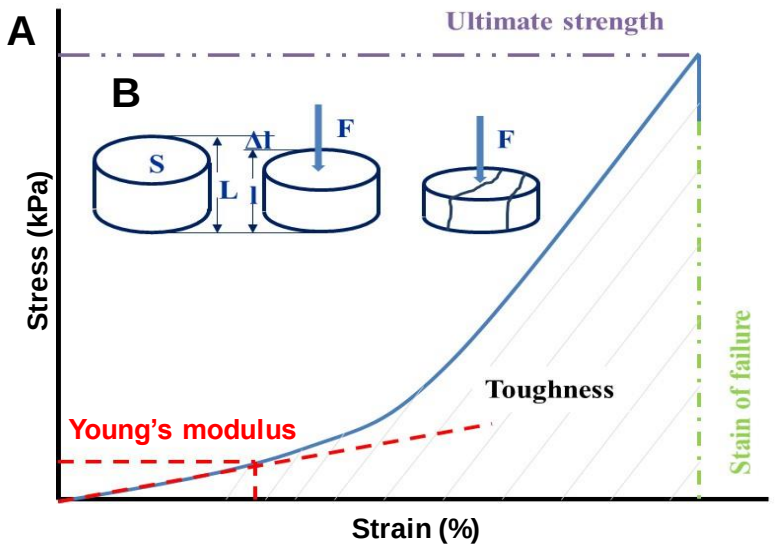

Figure 5: Several mechanical properties of a material can be quantitatively obtained from stress-strain curves. A. Schematic of how the mechanical properties are measured during gel compression up to gel failure. **B**. Example of stress-strain curve (dark blue) highlighting the modulus (diagonal red line), strain at failure (vertical dashed green line) and the ultimate strength (horizontal dashed purple line). The red dash lines are the examples of any arbitrary point at linear or elastic region which can be used to find the Young's modulus. S is surface area, L is initial height, Δl is dislocation, and F is applied force.

Pore interconnectivity was characterized using a water wicking test. Gel mass was measured before and after they were wicked with piece of tissue. The percent change in mass was recorded as the percent pore interconnectivity. The weight measurements were performed using an analytical balance (model AND SH-120). For detailed calculation please see appendix A.2.

The general microstructure of some of the macroporous cryogelated gels were assessed using scanning electron microscopy (SEM) (Zeiss SIGMA VP Field Emission). Gels were lyophilized immediately after cryogelation and placed on metal mounting post with adhesive and then sputter coated with platinum-palladium. Then, they were put in the SEM sample chamber and scanned to produce electron micrographic images.

2.4 Gel electrical characterizations

Gels were placed in the circuit similar to Figure 6. Voltage (8 volts) at different strains (0, 5, 30, 50, 75, and 90%) was applied (above the overpotential at the electrode/gel interface) and currents were recorded. Resistance, resistivity and electrical conductivity of the samples at 0% strain were calculated. Also conductances, at different strains (0, 5, 30, 50, 75, and 90 %) were calculated. For detailed calculation please see appendix A.3.

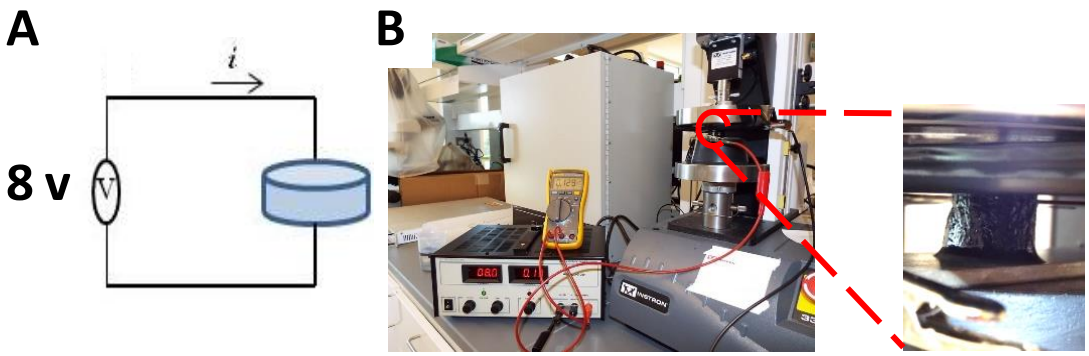

Figure 6. Electrical properties of each gel will be measured. A. Schematic of the electrical circuit used for recording the current. 8 volts is applied across a cylindrical gel (blue cylinder) and the current is measured. **B**. The set-up for recording the current under various strains with a zoomed-in image of a PEDOT cryogel under compression.

2.5 Gel characterizations after sterilization

In order to sterilize the hydrogel-based electrodes, they were soaked for a day in PBS then placed in 70% ethanol for an hour and then were swollen for another two days in sterile PBS to remove excess ethanol prior to being passed through a 16 gauge needle. As an alternative to ethanol sterilization, hydrogel-based electrodes were also sterilized using an autoclave. After removing gels from their molds, each gel was soaked in PBS in separate media bottles. Each media bottle was completely covered in aluminum foil and sealed with autoclave tape and autoclaved for 30 minutes (at 121 ℃). After

sterilization, in the manners described earlier (Sections 2.3 and 2.4), the electrical and mechanical properties of these injected gels were characterized and compared to those that were not sterilized. For detailed calculation please see appendix A.

2.6 Gel cyclic testing

In order to characterize gel robustness, gels were placed between the plates of an Instron (model 3345). Samples were cyclically loaded at 50% strain 10 times. Gels were also cycled 1 time at 90% strain in order to mimic the strain associated with injection. In the manners described in the sections 2.3 and 2.4 the mechanical and electrical properties of these gels were characterized and compared to those that were not cycled. For detailed calculation please see appendix A.

2.7 Gel injection

In order to investigate the injectability of gels, a subset of gels with desirable electrical and mechanical properties were made as described in section 2.2 at different sizes. These gels were cryogelated in 0.125 mm cylindrical Teflon molds with different (0.78, 1.08, 1.57, 2.35, and 3.14 mm) thicknesses. Then, cryogels were passed through 16 gauge needles and inspected afterwards for preservation of their structural integrity.

2.8 Data processing, representation, and statistical analyses

All data collected were represented as mean plus and minus standard deviations across repeat experiments. When comparing individual control single experimental conditions, student t-test was used to extract p-values. When comparing across multiple

conditions, Analysis of Variance (ANOVA) was employed with Tukey's post-hoc analysis. For all comparisons, a p-value of less than 0.05 was required as a benchmark for statistical significance.

3. Results and discussion

3.1 Characterizations of gels' mechanical properties

Mechanical compression experiments were performed to characterize how gel composition influenced mechanical properties such as stiffness, strain of failure, and toughness. Gels were made with different concentrations of polymer (poly(AAc)) and cross-linker (PEGDM) and a constant PEDOT concentration (2.6 wt %). This particular gel format was used to provide a negatively charged framework (poly (AAc) covalently cross-linked with PEGDM) for the conducting PEDOT to interpenetrate. 2.6 wt % PEDOT was the maximum concentration possible for all gel formulations and that in separate experiments, using higher PEDOT concentrations did not improve gel conductivity (data not shown). Additionally, it was thought that the electrostatic interactions between the positively charged PEDOT and the negatively charged AAc network would yield tough mechanical properties (Sun et al.). In these studies, it was found that increasing AAc and PEGDM concentrations increased gel stiffness (Fig. 7A and 7B, trendlines increasing from left to right). On the other hand, increasing AAc and PEGDM concentrations decreased strain of failure (Fig. 7C and 7D, trendlines decreasing from left to right), thus producing gels that, while stiffer, failed under lighter compression (i.e., were more brittle). Generally, cryogelation resulted in gels that were softer and could endure higher strains compared to their room temperature counterparts (Fig. 7A and 7B, comparing blue and red bars, particularly at higher cross-linking concentrations). This enhanced softness and strain at failure likely was due to the sponge-like macro-porosity exhibited by the cryogels (Fig. 7C). Note that often the softness of the cryogels was not characterized by the Young's modulus values. This

was likely due to the fact the highly macro-porous cryogels collapsed under their own weight and thus began compression tests in an already compressed (and therefore stiffer) state.

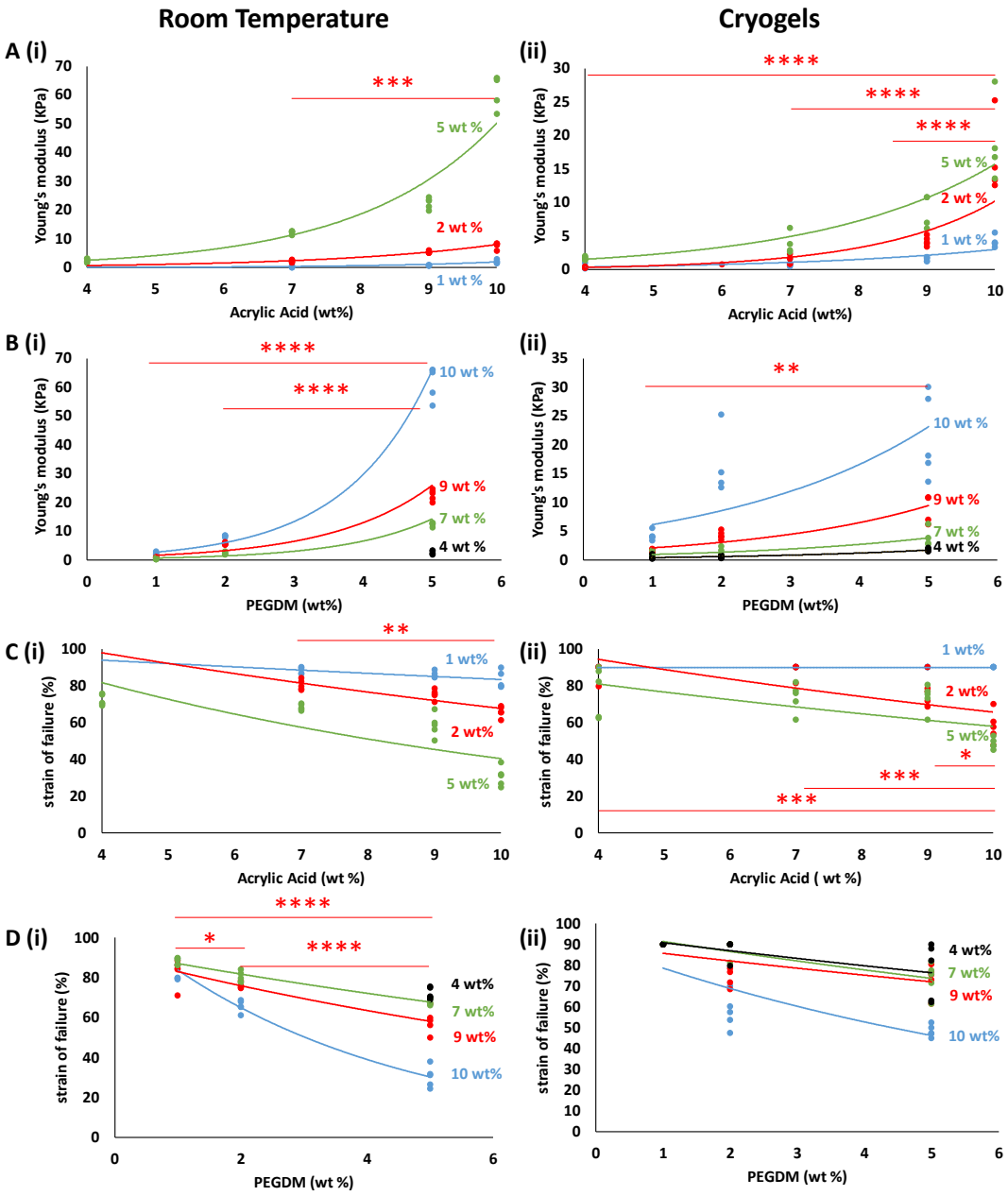

Figure 7. The strain of failure and stiffness of these 2.6 wt% PEDOT hydrogel-based electrodes are a function of hydrogel composition. A. Young's modulus as a function of AAc concentration for (i) gels cast at room temperature (RT) and (ii) gels that were cryogelated at -20 ℃. Blue, red and green data points and exponential trend lines corresponds to gels cross-linked using 1, 2, and 5 wt % PEGDM, respectively. **B.** Young's modulus as a function of PEGDM concentration for (i) gels cast at room temperature and (ii) gels were cryogelated at -20 ℃. Blue, red, green, and black data points trend lines correspond to gels with AAc concentration of 4, 7, 9, and 10wt %, respectively. **C.** Strain at failure as function of AAc concentration for (i) RT and (ii) cryogels. Blue, red, and green data points and trend lines correspond to gels cross-linked using 1, 2, and 5 wt% PEGDM, respectively. **D**. Strain of failure as a function of PEGDM concentration for (i) RT and (ii) cryogels. Blue, red, green and black data points trend lines correspond to gels with AAc concentration of 4, 7, 9, and 10wt %, respectively. In parts A through D, N = 4. *, **, ***, and **** indicate statistically significant differences when comparing gels of constant AAc concentration (A,B) or constant PEGDM concentration (C,D) with *p*-values of < 0.05, 0.01, 0.001, and 0.0001, respectively.

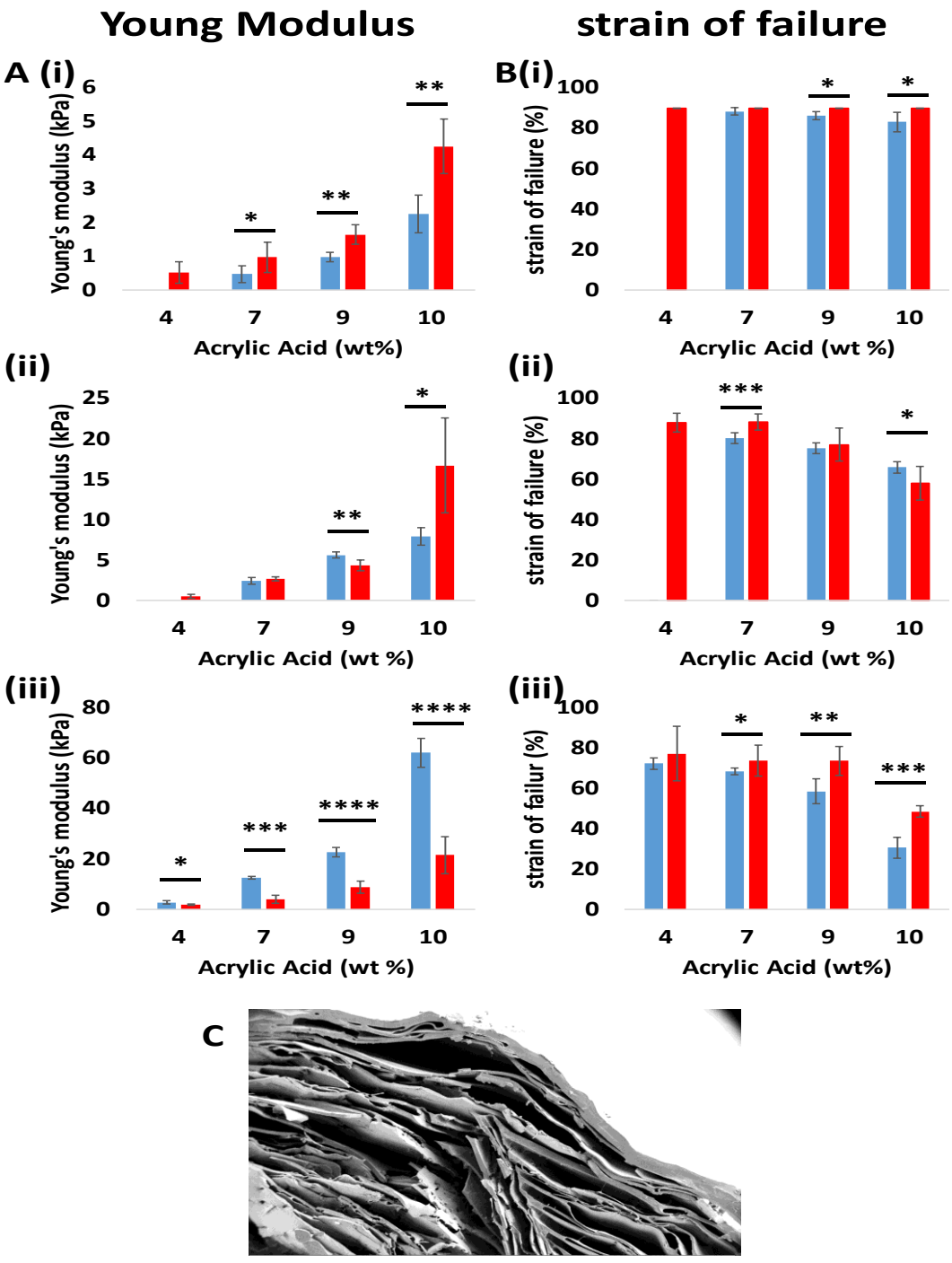

Figure 8. Cryogels were generally softer and could withstand higher strains than gels cast at room temperature. A. Bar graph comparing Young's moduli for gels cast at room temperature (blue) to cryogels (red) with PEGDM concentrations of (i) 1 wt %, (ii) 2 wt %, and (iii) 5 wt %. **B**. Bar graph comparing strain at failure for gels cast at room temperature (blue) to cryogels (red) with PEGDM concentrations of (i) 1 wt %, (ii) 2 wt %, and (iii) 5 wt %. **C**. An SEM image of a cryogel, highlighting its macro-porosity (for cryogel with 9 wt % AAc, 1 wt % PEGDM, 2.6 wt % PEDOT). In parts A and B, N = 4. *, **, ***, and **** indicate p-values of < 0.05, 0.01, 0.001, and 0.0001, respectively.

Gel toughness is a parameter related to both stiffness and strain of failure and is a mechanical parameter critical for injectability and long-term robustness. Generally, toughness increased with increasing Acrylic Acid and PEGDM concentration (Fig. 9A and 9B, trendlines increasing from left to right). Though this trend generally holds true, some gel formulations either did not follow this trend or only did so slightly. This might be a consequence of how increasing Acrylic Acid and PEGDM concentrations both increases stiffness (which allows the gels to absorbed more energy and small strains) but also increasing brittleness (which results in gels failing and lower strains). In other words, the mechanical toughness can likely be optimized at Acrylic Acid and PEGDM concentrations that are neither too high nor too low. In this work (as will be examined more in Section 3.3), we will be optimizing our gels for enhanced softness and ability to be injected. Namely, we will be looking for gels that have both low modulus and high strain of failure.

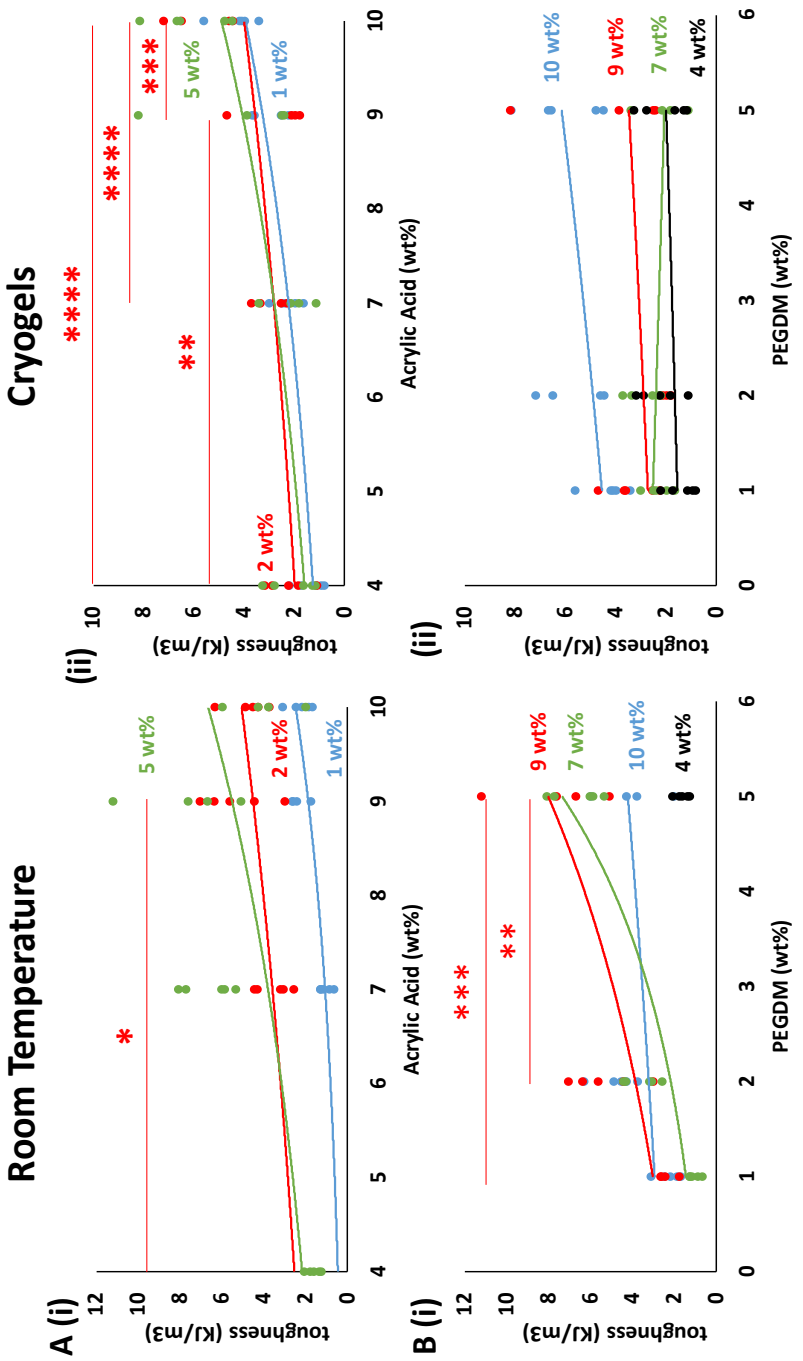

Figure 9. The mechanical toughness of these 2.6 wt % PEDOT hydrogel-based electrodes are a function of hydrogel gel composition. **A** Gel toughness as a function of AAc concentration for (i) RT and (ii) cryogels. Blue, red, and green data points and trend lines correspond to gels cross-linked using 1, 2, and 5 wt % PEGDM, respectively. **B** Gel toughness as a function of PEGDM concentration for (i) RT and (ii) cryogels. Blue, red, green, and black data points and trend lines correspond to gels with AAc concentrations of 4, 7, 9, and 10 wt %, respectively. N = 4. *, **, ***, and **** indicate p-values of < 0.05, 0.01, 0.001, and 0.0001, respectively, when comparing gels at constant AAc concentrations (A) or PEGDM concentrations (B).

The cryogelated PEDOT hydrogels developed here present several novelties in the area of electrically conductive hydrogels. First, to the best of our knowledge, these gels are the first instance of using PEDOT in the polymer form to create conducting hydrogels. The use of PEDOT described here enabled relatively rapid and straightforward gel fabrications. There have been reports of successful use of 3-4, ethylenedioxythiophene (EDOT) monomer (the monomer form of PEDOT) to form conducting hydrogels (Naficy et al.). In Naficy et al., EDOT was polymerized as a secondary network in and around a primary poly (Acrylic Acid) network to form a conducting hydrogel. However, the impact of different hydrogel formulations on gel mechanical properties was not examined. Critically, in our study, we have demonstrated the ability to explicitly tune gel mechanical properties by varying polymer and cross-linker concentrations. This ability to tune gel mechanicals will enable the use of conducting hydrogels in a wider range of applications, including applications that require injection of softer (tissue-like) neuroprosthetic electrodes. Second, to the best of our knowledge, the gels described here are the first reported use of a cryogelation approach to produce macro-porous PEDOT hydrogels with enhanced mechanical properties. Many gel formulations discovered here could with stand high degrees of compression while being relatively soft (Fig. 8, gels with > 90% strain of failure with moduli < 10 kPa). Naficy et al. created similar gels (PAA-PEDOT double network hydrogels at pH=6 with PEDOT concentrations of about 38 wt %) and reported stiffer gels (modulus about 90 kPa) and lower strain of failures (about 70 %). Elsewhere, Dai et al. fabricated gels with different concentrations of polymerized EDOT (8 - 18.4 wt %) with reported strain of failures ranging from 68 % to 78 %.

3.2 Characterization of gels' electrical properties

Electrical tests were performed to determine how gel composition influenced electrical conductivity. It was found that gel conductivity remained relatively constant for varying concentrations of AAc and PEGDM (Fig.10A and B, 0.8-1.2 S/cm for all gel formulations with no striking trends). This was likely due to the same amount of PEDOT concentration (2.6 wt %, the maximum possible concentration for the adopted fabrication process) being used in all gels. Higher PEGDM cross-linking did seem to slightly reduce conductivity (Fig. 9B, a slight downward trendline slope from left to right). We attributed this to several phenomena. First, gels with higher PEGDM cross-linking had lower pore interconnectivities (Fig. 10C, downward trend moving left to right, with this being more prominent in the macro-porous cryogels), therefore took on fewer conducting ions, and therefore did had slightly lower conductivities. Also, these highly cross-linked gels often bulged and did not make flush contact with the electrodes, again slightly reducing conductivity. In general, there were no strong trends between gel conductivity and gel composition, which suggests that the mechanical properties of these gels can be tuned (Figs. 7, 8, and 9) independently from their conductivities. Independence of conductivity from gel composition is beneficial, since it gives one the opportunity to choose gel composition based on the desirable mechanical properties determined by application, while retaining electrical conductivity. In any case, the conductivities exhibited by these PEDOT hydrogels were sufficient to light an LED with a battery (Fig. 10D), demonstrating relatively high conductivity.

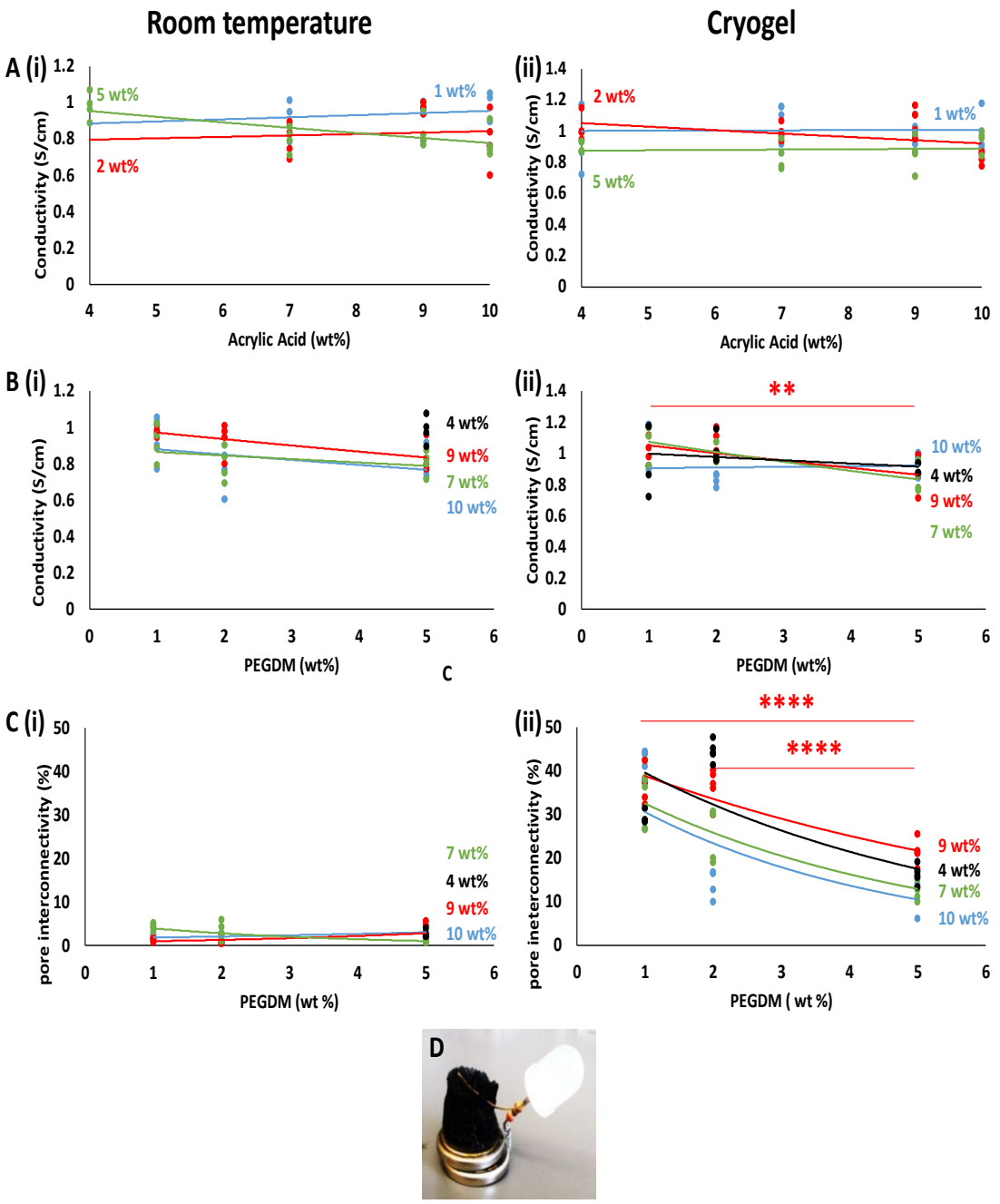

Figure 10. The electrical conductivity of these 2.6 wt % PEDOT gels does not dramatically vary based on AAc and PEGDM concentrations. **A** (i) RT and (ii) cryogelated gel conductivities at the indicated AAc concentrations for gels cross-linked using 1 (blue), 2 (red), and 5 (green) wt % PEGDM. **B** (i) RT and (ii) cryogelated gel conductivities at 1, 2, and 5 wt % PEGDM. 4 (black), 7 (green), 9 (red), and 10 (blue) wt% AAc. **C** (i) RT and (ii) cryogelated gel pore interconnectivity at 1, 2, and 5 wt % PEGDM. 4 (black), 7 (green), 9 (red), and 10 (blue) wt % AAc. **D** The conductivities provided by these PEDOT gels were sufficient to complete an LED circuit. Cryogel shown was made with 9 wt % AAc, 1 wt % PEGDM, and 2.6 wt% PEDOT. In part A, B, and C, N = 4. *, **, ***, and **** indicate statistically significant differences when comparing gels at constant AAc concentrations (A) or constant PEGDM concentrations (B, C) with p-values of < 0.05, 0.01, 0.001, and 0.0001 respectively.

While the electrical conductivities of these gels remained unaffected by AAc and PEGDM concentrations, certain Acrylic Acid and PEGDM formulations resulted in gels that were capable of providing enhanced electrical properties by virtue of their mechanical properties. Specifically, formulations that yielded softer gels could be compressed more readily and this compression resulted in enhanced electrical conductance. For example, under moderate strain (50%), softer, more compressible gels exhibited enhanced conductances compared to stiffer gels (Fig. 11, higher measured conductance for gels with lower Young's moduli in both RT and cryogels). This was likely due to compression reducing the electrical path. Interestingly, gels made at room temperature exhibited slightly higher conductances under moderate strain (50%) than macro-porous cryogels (comparing parts (i) and (ii) in Fig. 11A). This might be due to the differences in how non-macro-porous and macro-porous gels compress. Non-macro-porous room temperature gel volumes remained constant under compression: with reduction of height, gel surface area increased (Fig. 11B). This reduction in height and increase in cross-sectional surface area both enhanced electrical conductance. On the other hand, macro-porous cryogels tended to collapse in volume under compression: with reduction of height, surface area did not increase (the porous structure of the cryogels enabled this) (Fig. 11C). This type of collapse does enhance electrical conductance, but only due to reduction in height. Thus, macro-porous cryogels did not experience as much increase in conductivity when compressed. However, because this difference in conductance is only slight, and because the macro-porous cryogels exhibited excellent mechanics (softness and high strain of failure, Fig. 7), we believe they are more well-suited than PEDOT/EDOT gels (Naficy et al.; Dai et al. (2009); Dai

et al. (2010); Cho et al.; Saski et al.) as injectable soft electrode materials for neuroprosthetic interventions. Furthermore, the electrical properties of these macro-porous cryogels could be further enhanced using gel formations that resulted in higher degrees of pore interconnectivity. Specifically, cryogels with higher pore interconnectivity exhibited both higher conductivity at 0% strain (Fig. 12A, red data) and higher conductance at 50% strain (Fig. 12B, red data). Generally, cryogels could be made with higher pore interconnectivities by using formulations with modest amounts of AAc and PEGDM (i.e., formulations that utilized larger concentrations of water in lieu of polymer and cross-linker). This likely led to larger ice crystal development which promoted higher concentrations of PEDOT between ice crystals, leading to slightly higher electrical conductivity. Non-macro-porous room temperature gels, did not exhibit significant trends in this regard, likely due to their generally low pore interconnectivities (Fig. 12, blue data). Note that, again, while room temperature gels exhibited slighter higher conductances at 50% strain (Fig. 12A, blue data), these gels did not exhibit the high strain of failures required for injectability.

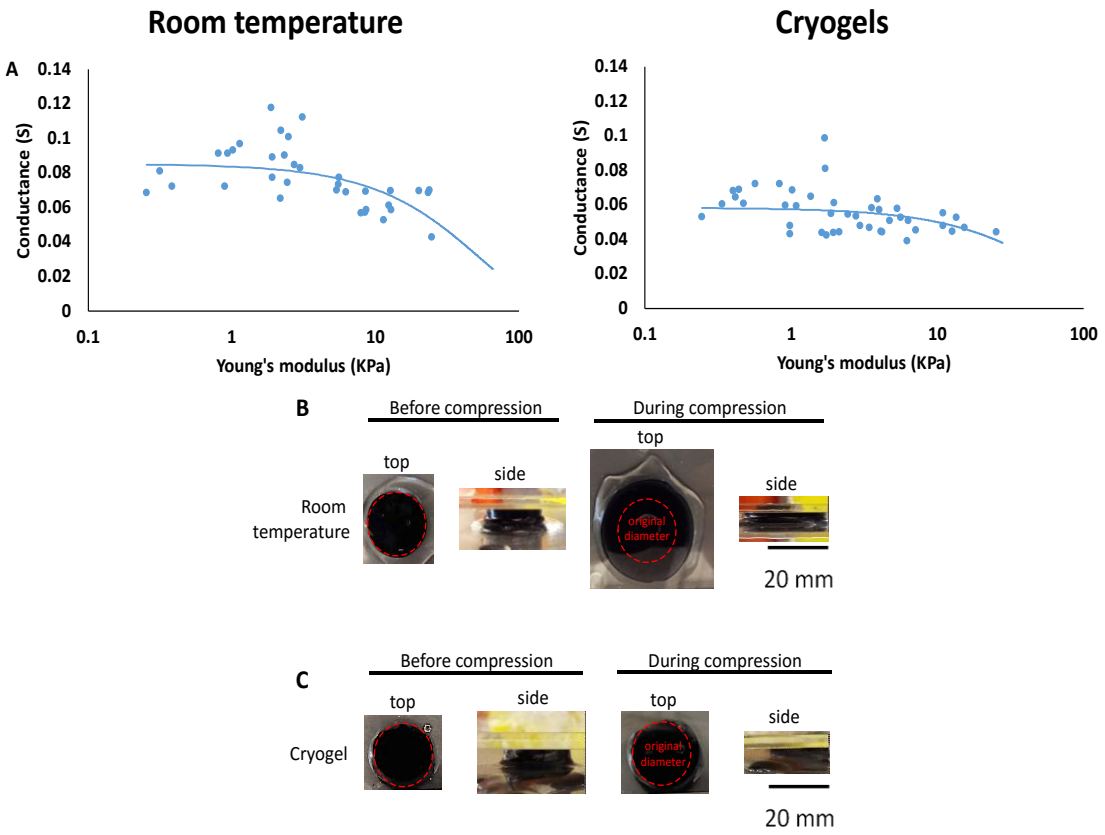

Figure 11. When compressed, softer gels exhibited enhanced electrical conductances. A. The measured conductance of (i) RT gels and (ii) cryogels as a function of their moduli at 50% strain. **B**. Photographs of room temperature made gels before and after compression, highlighting how the gel cross-sectional area increases during compression (thus enhancing conductance). **C**. Photographs of cryogels before and during compression, highlighting how gel cross-sectional area does not greatly increasing during compression.

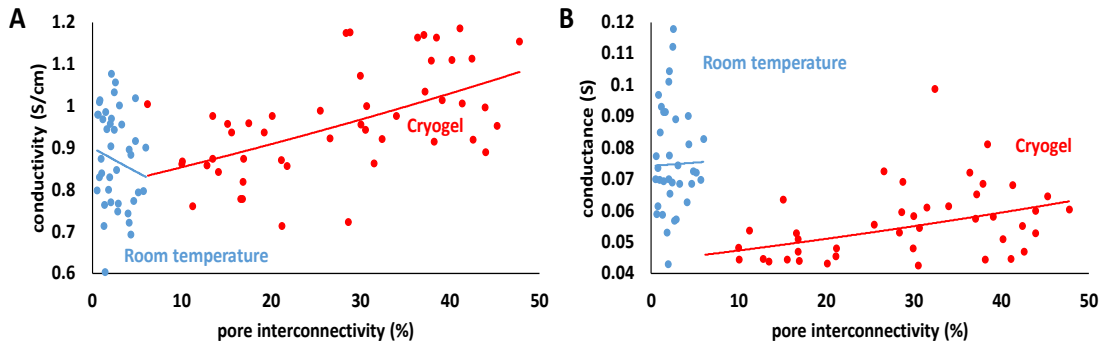

Figure 12. Cryogels with higher pore interconnectivities exhibited enhanced electrical conductivities and conductances. A. Conductivity (at 0% strain) as function of pore interconnectivity for RT gels (blue) and cryogels (red). **B.** Conductance at 50% strain as function of pore interconnectivity for RT gels (blue) and cryogels (red).

The PEDOT hydrogels reported here provide unique advantages for use in neuroprosthetic applications. First, despite the mechanical advantages discussed in the previous section, the electrical conductivities provided by these hydrogels are similar—if not better than—other reports. Using similar gels, Naficy et al. reported conductivities of 2.8 x 10^{-4} S/cm and 1 S/cm for single and double PAA-PEDOT network hydrogels, respectively. Elsewhere, dual PAA-PEDOT (8 – 18.4 wt % EDOT) networks similar to those described in Naficy et al. actually decreased in conductivity when compressed, with reported conductivities ranging from 6.7 x 10^{-4} to 1.2 x 10^{-3} S/cm (Dai et al. 2009). In another study conducted by Dai et al. (2010) using different hydrogel networks ((EDOT concentrations ranging from 0.48 to 1.2 mol/L) and polystyrene sulfonate (PSS) concentrations ranging from 0.1 to 1 mol/L) conductivities from 5.7 x 10^{-3} to 6.5 x 10^{-2} S/cm were reported (lower than here). In a separate study, Dai et al. (2010) went on to measure EDOT hydrogel conductivity with other formulations (0.03 to 0.48 mol/L EDOT and 0.1 to 0.5 mol/L PSS). Conductivity of these gels were reported to be 6.7 x 10^{-4} to 2.2 x 10^{-3} S/cm. Cho et al. reported conductivities ranging between 10^{-5} and 10^{-3} S/cm (when stimulated at 0.1 and 10^{6} kHz respectively at 25 ℃). One study (Saski et al.) was able to achieve enhanced conductivity between 40-80 S/cm by adopting a novel EDOT electropolymerized technique. However, this electropolymerization technique is more appropriate for thin film hydrogels or hydrogels as coatings. The electrical conductivities reported here and in these other studies (Naficy et al.; Dai et al. 2009; Dai et al. 2010; Cho et al.; Saski et al.) are likely appropriate for electrical stimulation and sensing of neural tissues. For instance, because brain tissue is about 0.0015 to 0.003 S/cm and cerebrospinal fluid is about 0.015 S/cm (Lorenzo et al.), neuroprosthetic

electrode materials must exhibit higher conductivities for proper sensing/stimulation. Our hydrogel-based electrodes (and some of those cited here) provide electrical conductivities well above these tissues and fluids (Figs. 10 and 12). Notably, however, our PEDOT cryogels provide the mechanical properties required for minimally invasive injection *in addition* to adequate electrical conductivities. While electrically conducting injectable hydrogels have been reported previously, they were fabricated with completely different materials (gelatin-based) using different fabrication methods, and only yielded conductivities around 7.25×10^{-3} S/cm (Li et al.)

3.3 Optimization of gel mechanical and electrical properties

Because of the complex interplay between gel composition and the many parameters of interest here (Young's modulus, strain of failure, toughness, and electrical conductivity), we have directly measured each of these parameters over a wide range of gel formulations. This has allowed us to identify select gel formulations that provide both desirable mechanical and electrical properties for use as injectable, conducting, and soft neuroprosthetic electrodes. In order to obtain relatively soft gels, only gels with stiffness less than 2 kPa were chosen (Fig 13A, bars identified with diamonds). Also for injectability, gels must be passed through 16 gauge needles and therefore should tolerate high strains. Thus, only gels which did not show any sign of failure at 90% strain were selected (Fig. 13B, bars identified with daggers). For long-term survival robustness and mechanical toughness are critical parameters. Thus, only gels which could absorb energy more than 2 kJ/m^3 were selected (Fig. 13C, bars identified with double daggers). Finally, in order to receive and deliver electrical signals in neuroprosthetic applications, only the most conductive gels were desirable. Thus, only gels which had at least 1 S/cm conductivities were selected (Fig. 13D, bars identified with lightning bolts). The only gels that satisfied all these requirements were the 7 wt % AAc, 1 wt % PEGDM cryogels and the 9 wt % AAc, 1 wt % PEGDM cryogels (both containing 2.6 wt % PEDOT). These optimized gels could both survive high strains (Fig. 14A and B) and exhibited excellent electrical conductance under this high strain (Fig. 14C). In fact, the electrical conductance of gels when compressed from 0 to 90 % strain increased by an order of magnitude (Fig. 14C). This property may be very useful when these cryogels are compressed within tissue after injection and the electrode conductance may increase.

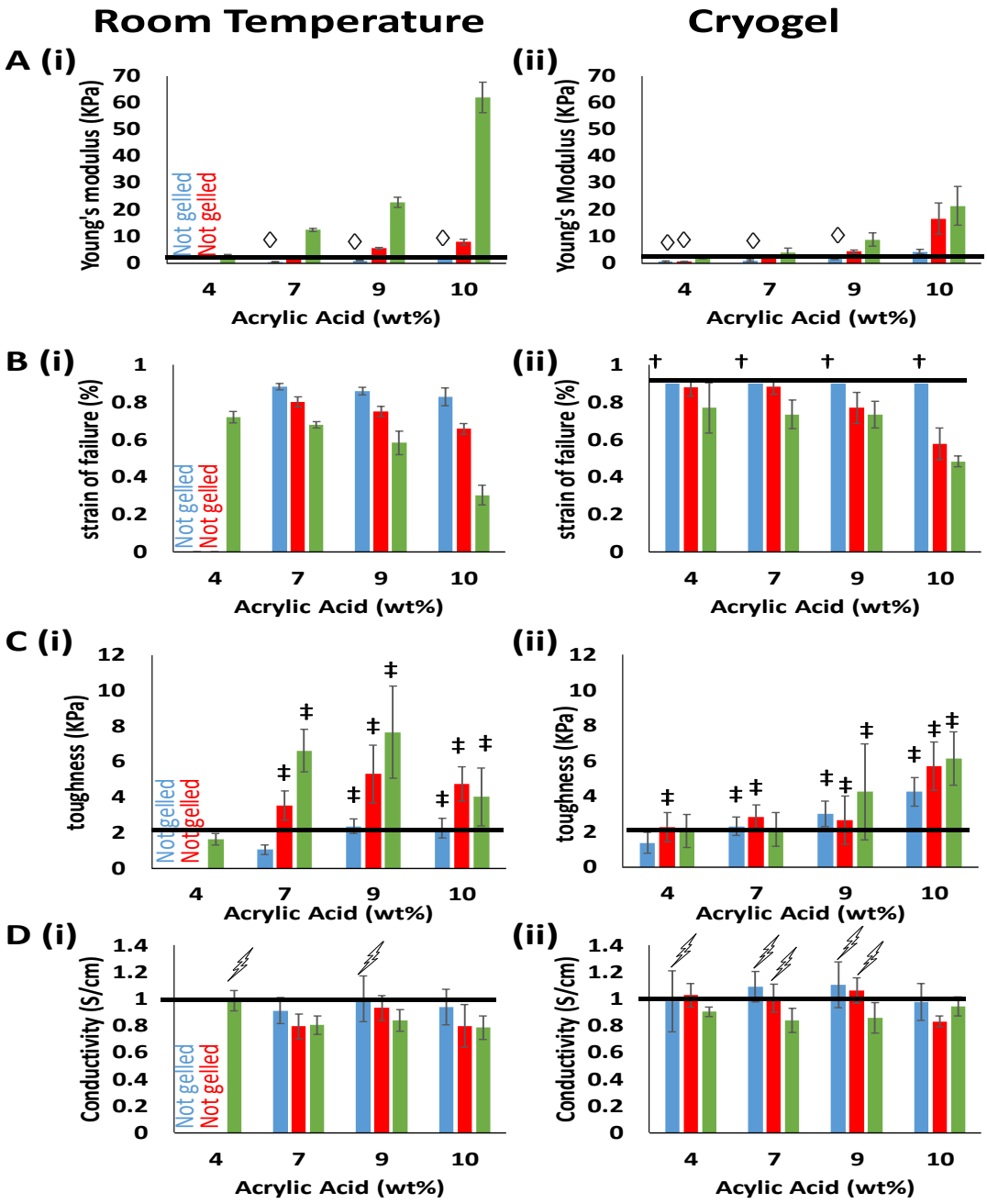

Figure 13. Gels with both desirable mechanical and electrical properties can be identified. **A** Young's modulus vs. AAc concentration for 2.6 wt % PEDOT gels cross-linked using 1 (blue), 2 (red), and 5 (green) wt % PEGDM. Diamonds indicate gels that had Young's moduli above 2 kPa. **B** Strain of failure vs. AAc concentration for 2.6 wt % PEDOT gels cross-linked using 1 (blue), 2 (red), and 5 (green) wt % PEGDM. Daggers indicate gels that had strain of failures of at least 90%. **C** Gel toughness vs. AAc concentration for 2.6 wt % PEDOT gels cross-linked using 1 (blue), 2 (red), and 5 (green) wt % PEGDM. Double daggers indicate gels that absorbed at least 2 kJ/m^3 before failure. **D** Gel electrical conductivity vs. AAc concentration for 2.6 wt % PEDOT gels cross-linked using 1 (blue), 2 (red), and 5 (green) wt % PEGDM. Lightning bolts indicate gels with conductivities of at least 1 S/cm.

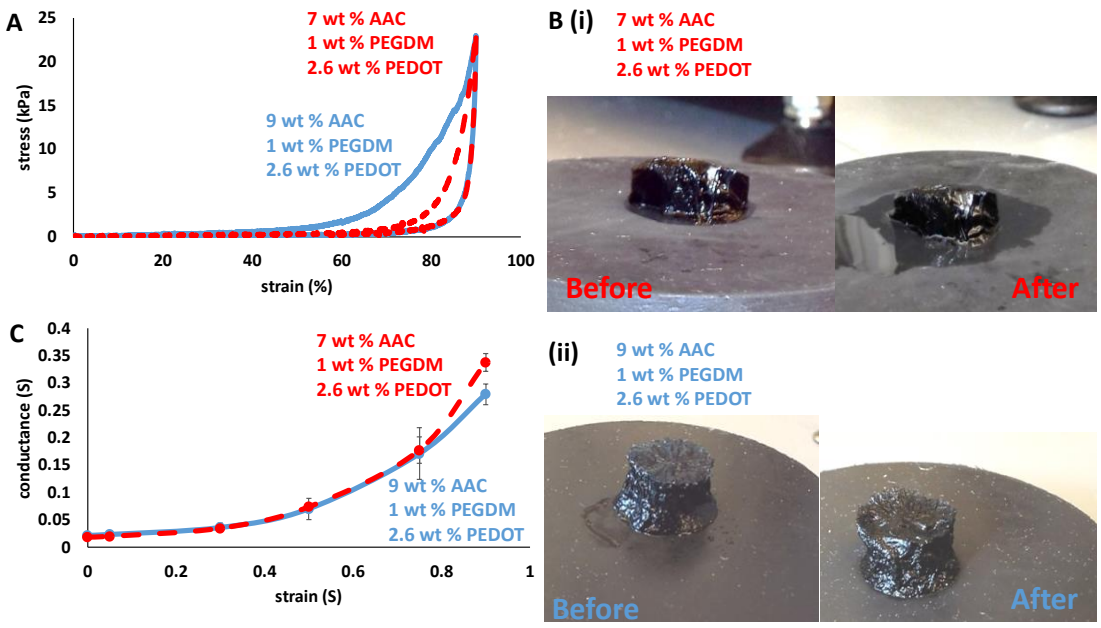

Figure 14. Optimized gels could survive high strains and exhibited enhanced conductances under this strain. **A** Stress-strain curves of a full cycle for 9 wt % AAc, 1 wt % PEGDM, and 2.6 wt% PEDOT gels when compressed to 90%. **B** Photographs of the PEDOT cryogel used in part A before and after one 90% cycle for 7 wt % AAc, 1 wt % PEGDM, 2.6 wt% PEDOT (i) and 9 wt % AAc, 1 wt % PEGDM, 2.6 wt% PEDOT (ii) gels. **C** Electrical conductance as a function of strain for 7 wt % AAc, 1 wt % PEGDM, 2.6 wt% PEDOT (red) and 9 wt % AAc, 1 wt % PEGDM, 2.6 wt% PEDOT (blue) gels.

3.4 Gel properties when cyclically compressed, sterilized, and injected

For use in neuroprosthetic applications, these hydrogel materials must be robust enough to retain their mechanical and electrical properties after cyclic compression and sterilization. As injectable electrode materials, they must also remain structurally intact when subjected to the high strains associated with injection. We therefore conducted experiments examining how cyclic compression and sterilization influenced gel electrical and mechanical properties and directly tested these gels for injectability. After selecting optimum cryogel formulations (7 and 9 wt % AAc, 1 wt % PEGDM, and 2.6 wt % PEDOT), they were sterilized with ethanol or in an autoclave. Results indicated that ethanol-sterilization had less effect on gel mechanical properties than autoclave-sterilization. Specifically, Young's modulus moderately changed after ethanol treatment (Fig. 15A, "ethanol" column) whereas autoclave treatment significantly altered the modulus (Fig. 15A, "autoclave" column). This was most prominent in the 9 wt % AAc cryogels (Fig. 15A, blue bars). Additionally, autoclaving gels increased stiffness, which is not desirable for this application. Most critical to injection, however, is that ethanol treated gels fully retained their ability to undergo large strains (Fig. 15B, "ethanol" column) while autoclaved gels did not. Furthermore, ethanol-sterilized gels retained their mechanical properties better after cyclic compression (Fig. 15A and B, "ethanol + 10 cycle" and "autoclave + 10 cycle" columns). Taken altogether, these data indicate that autoclaving might change the structure of these gels, increasing their stiffness and eliminating their shape memory properties. Thus, ethanol treatment appears to be a more desirable method for sterilizing these gels.

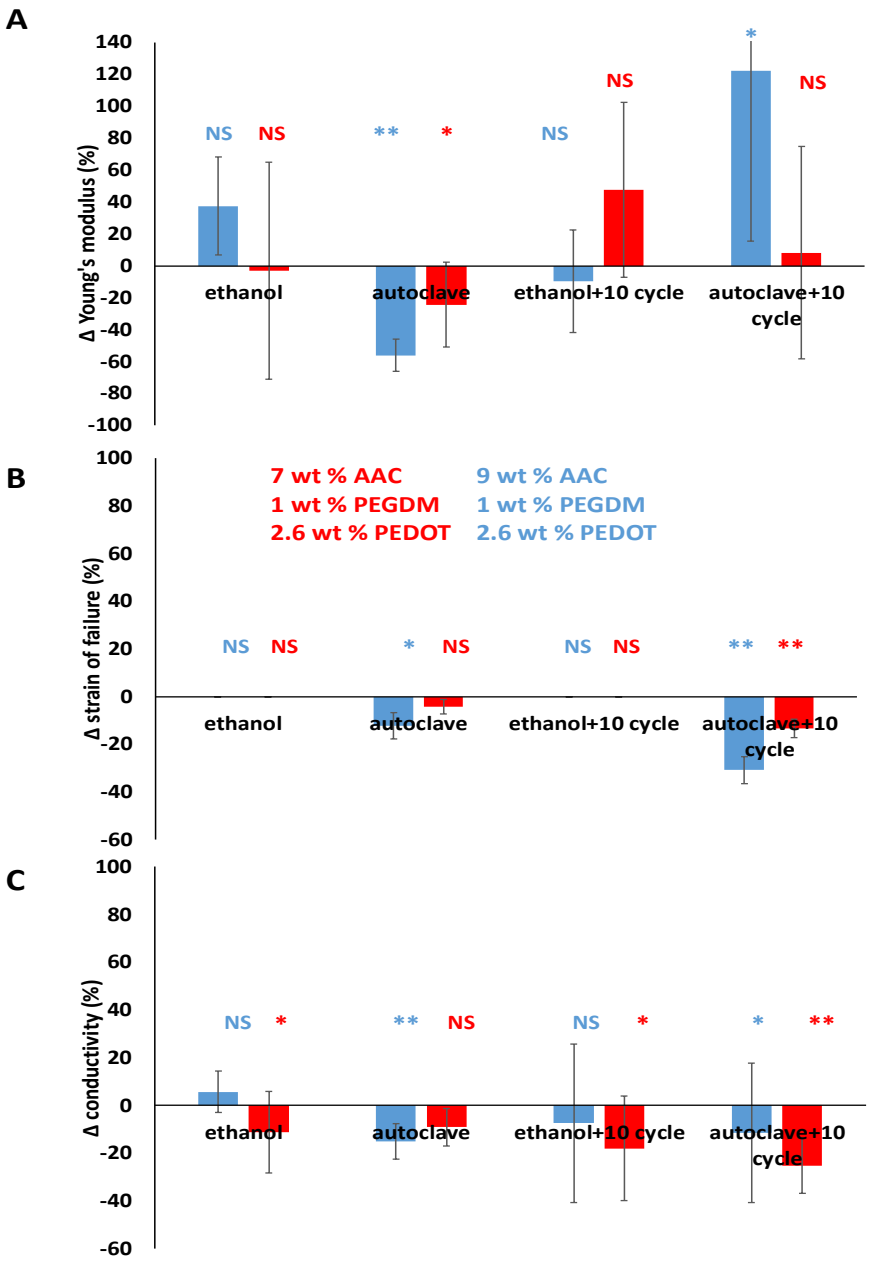

Figure 15. The method of sterilization determines if these gels' mechanical and electrical properties are preserved. (A). Percent change of Young's modulus after sterilization with ethanol, autoclave, and after 10 cycles for both ethanol- and autoclave-treated cryogels. (**B**). Percent change of strain of failure after sterilization with ethanol, autoclave, and after 10 cycles for both ethanol-l and autoclave- treated cryogels. (**C**). Percent change of conductivity after sterilization with ethanol, autoclave, and after 10 cycle for both ethanol- and autoclave-treated for cryogels. For parts A through C, 9 wt % AAc, 1 wt % PEGDM, and 2.6 wt % PEDOT cryogels are represented by blue bars and 7 wt % AAc, 1 wt % PEGDM, and 2.6 wt % PEDOT cryogels are represented by red bars. N = 4. * and ** indicate statistical differences with p-values of < 0.05 and 0.01, respectively, when comparing before and after values of moduli (A), strain of failure (B), and conductivity (C). n.s. indicates no statistical significance ($p > 0.05$).

Testing the electrical conductivity after sterilization and cyclic testing also revealed some interesting insights. Surprisingly, sterilization moderately improved conductivity, except for the ethanol-treated 9 wt % cryogels (Fig. 15C, bars indicating positive percent changes). Although 9 wt % cryogels sterilized with ethanol electrical conductivity slightly increased, this result did not occur after ten cycles (Fig. 15C, "ethanol + 10 cycles" column, blue bar). These increases in electrical conductivity likely are due to both ethanol- and autoclave-treatments changing the macro-porous gel structure. For instance, ethanol-treatment causes these gels to collapse greatly, forcing macro-pores to close. Autoclave-treatment likely damages the gels, also forcing macro-pores to collapse. In both cases, this pore closure likely increased electrical conductivity (i.e., better interconnectivity of the conducting hydrogel when pore walls touch). While these increases in electrical conductivities may be desirable, they are likely temporary—especially for the ethanol-treated gels, since the de-swelling effects of ethanol treatment may not persist after being subjected to physiological media for prolonged periods of time.

In order to verify injectability, both optimized gels (7 and 9 wt % AAc, 1 wt % PEGDM, and 2.6 wt % PEDOT cryogels) were passed through 16 gauge needles. Success of injection (Fig. 16A) was dependent on the speed of injection, size of cryogel, and how well hydrated the gels were. As expected, cryogels with smaller diameters survived injection better than larger gels (Fig. 16B). Notably, gels made with 9 wt % Acrylic Acid, 1 wt % PEGDM, and 2.6 wt % PEDOT survived injection better than the 7 wt % Acrylic Acid cryogels (Fig. 16B, red bars only surviving at appreciable rates for gels < 1.28 mm thick, whereas blue bar indicate 100% survival of 1.58-mm-thick gels).

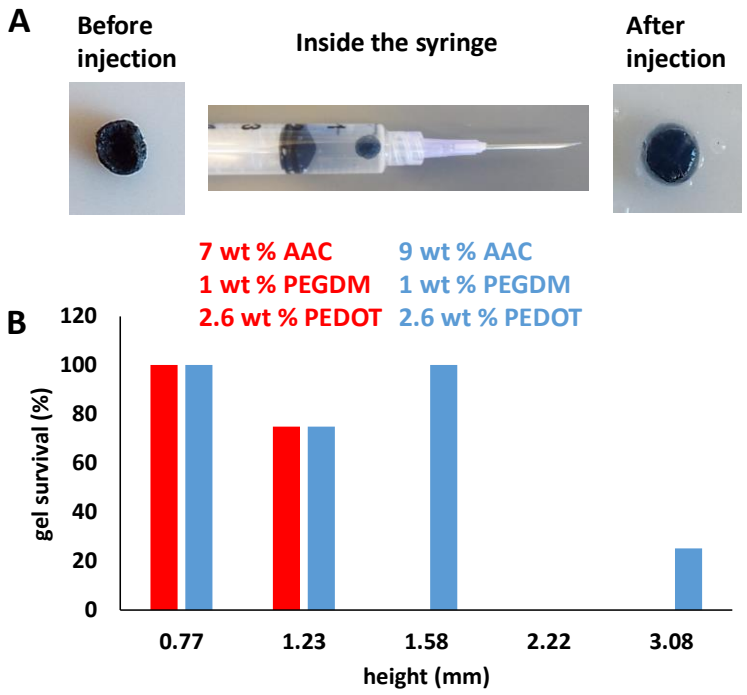

Figure 16. These gels are injectable with some gel sizes working better than the others. A Different stages of injection before injection, inside the syringe, and after injection. **B** Gel survival percentage as a function of height for diameter = 0.125 mm for cryogels 7 wt% AAc, 1 wt % PEGDM, 2.6 wt % PEDOT (red) and 9 wt% AAc, 1 wt % PEGDM, 2.6 wt % PEDOT (blue).

There are other efforts to create injectable conducting hydrogels, though using different approaches to fabricate the hydrogels. Li et al. (2014) adopted an in situ crosslinking approach to form gelatin-graft-polyaniline (GP) gels at body temperature. The solution was injected to animal hosts, and introduction to body temperature initiated gel polymerization. Conductivity of these gels was reported to be several orders of magnitude lower than those reported in the present study (between 1.21×10^{-4} – 4.45×10^{-4} S/cm). Also, Li et al. (2014) reported swelling ratios that significantly increased over time after in situ injection (up to 500 %), which could be highly problematic in that this swelling could damage sensitive neural tissues. The optimized cryogels reported in

our study swelled only 33.25 % and 36.75 % (7 wt % AAc, 1 wt % PEGDM, 2.6 wt % PEDOT and 9 wt % AAc, 1 wt % PEGDM, 2.6 wt % PDOT, respectively). The GP hydrogels reported by Li et al. (2014) also degraded and lost over 95% of their weight in 22 days, making them useful in many applications, but not well-suited for long-term electrode-neural interfaces. The optimized cryogels reported here were not designed to degrade and remained intact for several months in vitro. In another study (Li et al. (2015)), conductive hydrogels were made of gelatin-graft-polyanaline (GP) and carboxymethyl-chitosan, and in situ crosslinked with oxidized dextran via Schiff base at physiological conditions. These gels also gelated after injection and exhibited improvements in both electrical conductivity and swelling ratio from Li et al. (2014). Increasing the amount of polyanaline reduced swelling ratio down to 120%. Conductivity of these gels were improved (increased from 6.2×10^{-3} S/cm to 7.3×10^{-3} with increasing polyaniline), but were still orders of magnitude lower than what are reported in the present study. Elsewhere, Wu et al. adapted host-guest interactions to fabricated hydrogels. Hydrogels were used γ-cyclodextrin dimers as the host molecule and tetraaniline and poly (ethylene glycol) as the guest copolymer, enabling gelation post injection. While utilizing a highly novel gelation approach, the conductivity of these gels was in the range of 10^{-4} S/cm. Our gels had comparatively higher conductivities (about 1 S/cm).

4. Conclusion

We were able to generate electrically conducting hydrogels with unique mechanical properties by interpenetrating a PEDOT network with a poly (acrylic acid) network. The gels' mechanical properties could be tuned (1 to 70 kPa) by altering the amount of both poly (acrylic acid) polymer and PEGDM cross-linker contained in the gel. Notably, altering gel composition in order to achieve tuned mechanics did not overly affect gel conductivity (maintained around 1 S/cm). Cryogelation of these conducting gels produced gels that were very soft (< 10 kPa) and exhibited excellent strain of failures (> 90%) and mechanical toughness (2 – 8 kJ/m^3). Owing to these enhanced mechanical properties, specific gel formulations (7 and 9 wt % AAc with 1 wt % PEGDM and 2.6 wt % PEDOT) were identified to be highly compressible and proved to be capable of sterilization (ethanol-treatment), cyclical compression, and injection through a 16-gauge needle. Also, owing to this compressibility, when compressed, these gels exhibited enhanced electrical conductances. We believe the combination of softness, toughness, compressibility, and electrical conductivity exhibited by these PEDOT-based hydrogels make them very well suited for use in neuroprosthetic applications where injectability and softness are desirable material attributes for minimizing inflammation, reducing scar tissue, and prolonging electrical contact with neural tissues.

5. Bibliography

Abidian, M. R.; D. H. Kim; D. C. Martin; 'Conducting polymer nanotubes for controlled drug release'; *Advanced Materials*; 2006; 18(4); pp 405-409

Abidian, M. R.; D. C. Martin; 'Experimental and theoretical characterization of implantable neural microelectrodes modified with conducting polymer nanotubes'; *Biomaterials* (29); 2008; pp 1273-1283

Aregueta-Rables, U. A.; A. J. Woolley; L. A. Poole-Warren; N. H. Lovell; R. A. Green; 'Organic electrode coatings for next-generation neural interfaces'; *Frontiers in Neuroengineering*; 2014; volume 7; Article 15

Asplund, M.; T. Nyberg; O. Inganäs; 'Electroactive polymer for neural interfaces'; *Polymer Chemistry*; 2010; 1; pp 1374-1391

Bencherif, S. A.; R. W. Sands; D. Bhatta; P. Arany; C. S. Verbeke; D. A. Edwards; D. J. Mooney; 'Injectable performed scaffolds with shape-memory properties'; *Proceedings of National Academy of Sciences of United States of America;* 2012; 109 (48); pp 19590-19595

Carmel, J. B.; H. Kimura; L. J. Berrol; J. H. Martin; 'Motor cortex electrical stimulation axon growth to Brain stem and spinal targets that control the forelimb impaired by unilateral corticospinal injury'; *European Journal of Neuroscience*; 2013; 37(7); pp 1090-1102

Cezar, C. A.; S. M. Kennedy; M. Mehta; J. C. Weaver; L. Gu; H. Vandenburgh; D. J. Mooney; 'Biphasic ferrogels for triggered drug and cell delivery'; *Advanced Healthcare Materials*; 2014; 3(11); pp 1869-1876.

Cheong, G. I. M.; K. S. Lim; A. Jakubowicz; P. J. Martens; L. A. Poole-Warren; R. A. Green; 'Conductive hydrogels with tailored bioactivity for implantable electrode coatings'; *Acta Biomaterialla;* 2014; 10; pp 1216-1226

Chen X.L.; Y.Y. Xiong; G.L. Xu; X.F. Liu; 'Deep brain stimulation'; *Intervention Neurology*; 2012; 1; pp 200-212

Cho, W.; J. Wu; B. S. Shim; W. F. Kuan; S. E. Mastroianni; W. S. Young; C. C. Kuo; T. H. Epps; D. C. Martin; 'Synthesis and characterization of biocontinuous cubic poly (3,4-ethylene dioxthiophene) gyroid (PEDOT GYR) gels'; *Physical Chemistry Chemical Physics.*; 2015; DOI: 10.1039/c4cp04426f

Cogan, S. F.; 'Neural stimulation and recording electrodes'; *Annual Review of Biomedical Engineering*; 2008; 10; pp 275-309

Cunha, C. D.; S. L. Boschen; A. Gomez-A; E. K. Ross; W. S. J. Gibson; H. K. Min; K. H. Lee; C. D. Blaha; 'Toward sophisticated basal ganglia neuromodulation: review on basal ganglia deep barin stimualtion'; *Neuroscience and Biobehavioral Review*; in press

Dai, T.; Qing, X.; Lu, Y.; Xia, Y. 'Conducting hydrogel with enhanced mechanical strenght'; *Polymer*; 2009; 50; pp 5236-5241

Dai, T.; Qing; X.; H. Zhou; C. Shen; J. Wang, J; Y. Lu; 'Mechanically strong conducting hydrogel with special double-network structure'; *Synthetic Metals*; 2010; 160; pp 791-796

Dai, T.; Shi; S. Zhiquan; C. Shen; J. Wang;Y. Lu; 'Self-strengthened conducting polymer hydrogels'; *Synthetic Metals*; 2010; 160; pp 1101-1106

Dee, K. C.; D. A. Puleo; R. Bizios; *An introduction to tissue-Biomaterial interactions*; Hoboken; NJ; John Wiley and Sons; 2002

Dilorenzo, D.J.; J.D. Bronzino; 2008; *Neuroengineering*; Boca Raton; Fl; *CRC Press*

Elliott, J. E.; M. Macdonald; J. Nie; C. N. Bowman; 'Structure and swelling of poly (acrylic acid) hydrogels: effect of pH, ionic strength, and dilution on the crosslinked polymer structure'; *Polymer*; 2004; pp 1503-1510

Engler A. J.; S. Sen; H. L. Sweeney; D. E. Discher; 'Matrix elasticity directs stem cell linage specification'; *Cell;* 2006; 126; pp 677-689

Ertürk, G.; B. Mattiasson; 'Cryogels-versatile tools in biosepration'; *Journal of Chromatography A'*; 2014; 1357; pp 24-35

Fattahi, P.; G. Yang; G. kim; M.R. Abidian; 'A review of organic and inorganic biomaterials for neural interfaces'; *Advanced Materials*; 2014; vol. 26; no. 12

Fridman, G. Y.; Charles C. D. Santina; 'Progress toward development of multichannel vestibular prosthesis for treatment of bilateral vestibular deficiency'; *The Anatomical Record*; 2012; 295 (11); pp 2010-2029

Green, R. A.; C. M. Williams; N. H. Lovell; L. A. Poole-Warren; 'Novel neural interface for implant electrodes: improving electroactivity of polypyrrole through multi-walled carbon nanotube incorporation'; *Journal of Material Science: Material Medicine*; 2008; 19; pp 1625-1629

Green, R. A.; H. Toor; C. Dodds; Nigel H. Lovell; 'Variation in performance of platinum electrode with size and surface roughness'; *Sensors and Materials*; 2012; volume 24; no 4; pp 165-180

Guimard, N. K.; N. Gomez; C. E. Schmidt; 'Conducting polymers in biomedical engineering'; *Progress in Polymer Science*; 32 (2007) 876-921

Guiseppi-Elie, A.; 'Electroconductive hydrogels: Synthesis, characterization and biomedical applications'; *Biomaterials*; 2010; 31; pp 2701-2716

Gulyuz, U.; O. Okuy; 'Self-healing poly (acrylic acid) hydrogels with shape memory behavior of high mechanical'; *Macromolecules*; 2014; 47; 6889-6899

Gun'ko, V. M.; I.N. Savina; S. V. Mikhalovsky; 'Cryogels: morphological, structural and adsorption characterisation'; *Advances in Colloid and Interface Science'*; 2013; 187-188; pp 1-46

Hammond, C.; R. Ammari; B. Bioulac; L. Garcia; 'Latest views on the mechanisms of action of deep brain stimulation'; *Movement Disorders*; 2008; volume 23; issue 15; pp 2111- 2121

Hassarati, R. T.; W. F. Dueck; C. Tasche; P. M. Carter; L. A. Poole-Warren; R. A. Green; 'Improving Cochlear implant properties through conductive hydrogel coating'; *IEEE Transactions on Neural Systems and Rehabilitation Engineering*; 2014; volume 22; no 2

Huang, P.; W. Chen; L. Yan; 'An inorganic-organic double network hydrogel of grapheme and polymer'; *Royal Society of Chemistry: Nanoscale*; 2013; volume 5; pp 6034-6039

Kenendy, S.; S. Bencherif; D. Norton; L. Weinstock; M. Mehta; D. Mooney; 'Rapid and extensive collapse from electrically responsive macroporous hydrogels'; *Advanced Healthcare Materials*; 2014; volume 3; issue 4; pp 500-507

Kumar, A.; A. Sirvastava; 'Cell separation using cryogel-based affinity chromatography'; *Nature Protocols*; 2012; 5; pp 1737-1747

Kuo, J.R.; S.S. Lin; J. Liu; S.H. Chen; C.C. Chio; J.J. Wang; J.M. Liu; 'Deep brain light stimulation effects on glutamate and dopamine concentration; *Biomedical Optic Express*; 2014; vol. 6; no. 1

Leach, J. B.; A. K. H. Achyuta; S. K. Murthy; 'Bridging the divide between the Neuroprosthetic design, tissue engineering and neurobiology'; *Frontiers in Neuroengineering*; 2010; volume 2; article 10

Li, L.; J. GE; P. X. Ma; B. Guo; 'Injectable conducting interpenetrating polymer network hydrogels from gelatin-graft-polyaniline and oxidized dextran with enhanced mechanical properties'; *RSC Adv*; 2015; 5; 92490 (accepted 15 th October 2015)

Lin-Gibson, S.; S. Bencherif; J. A. Cooper; S. J. Wetzel; J. M. Antonucci; B. M. Vogel; F. Horkay; N. R. Washburn; 'Synthesis and characterization of PEG dimethyacrylate and their hydrogel'; *Biomacromolecules*; 2004; 5; pp 1280-1287

Lorenzo, A. M.; Hallet, M; (2013); 'Handbook of clinical neurology, vol. 116 (3rd series) brain stimulation', *Elsevier, B. V.*

Lu, Y; W. He; T. Cao; H. Guo; Y. Zhang; Q. Li; Z. Shao; Y. Cui; X. Zhang; 'Elastic, conductive, polymeric hydrogels and sponges'; *Scientific Reports*; 2014; 4: 5792; DOI: 10.1038/srep05792

Lyons, M. K.; 'Deep brain stimulation Current and future application'; *Mayo Clinic Proceedings*; 2011; 86; 7; pp 662-672

Martin, D. C.; J. Wu; C. M. Shaw; Z. King; S. A. Spanninga; S. Richardson-Burns; J. Hendricks; J. Yang; 'Morphology of poly (3,4-ethylenedioxythiophene)'; *Polymer Reviews*; 50; 3; pp 340-384; DOI: 10.1080/15583724.2010.495440

McIntyre, C. C.; A. Chaturvedi; R. R. Shamir; S. F. Lempka; 'Engineering the next generation of clinical deep brain stimulationtechnology'; *Brain Stimulation*; 2015; 8:21-26

Merril, D. R.; M. Bikson; J. G. R. Jefferys.; 'Electrical stimulation of excitable tissue: design of efficacious and safe protocols'; *Journal of Neuroscience Methods*; 2005; 141; pp 171-198

Minassian, K.; U. Hofstoetter; K. Tansey; W. Mayr; 'Neuromodulation of lower limb motor control in restorative neurology'; *Clinical Neurology and Neurosurgery*; 2012; 114; 5; pp 489-497

Naficy, S.; J. M. Razel; G. M. Spinks; G. G. Wallace; P. G. Whitten; 'Electrically conductive, tough hydrogels with pH sensitivity'; *Chem. Mater.*; 2012; 24; pp 3425-3433

Pan, L.; G. Yu; D. Zhai; H. R. Lee; W. Zhao; N. Liu; H. Wang; B. C. K. Tee; Y. Shi; Z. Bao; 'Hierarchial nanostructured conducting polymer hydrogel with high electrical activity'; *Proceedings of National Academy of Sciences of the United States of America*; 2012; vol. 109; no. 24; pp 9287-9292

Paffi, A.; F. Camera; F. Apollonio; G. d'Inzeo; M. Liberti; "Numerical characterization intraoperative and chronic electrodes in deep brain stimulation"; *Frontiers in Computational Neuroscience*; 2015; doi: 10.3389/fncom.2015.00002

Pezaris, J. S.; E. N. Eskandar; 'Getting signals to brain: visual prosthetics through thalamic microstimulation'; *Neurosurgical Focus*; 2009; 27;1

Pilate, F.; R. Mincheva; J. De Winter; P. Gerbaux; L. Wu; R. Todd; J. M. Raquez; P. Dubios; 'Design of multistimuli-responsive shape-memory polymer materials by reactive extrusion'; *Chemistry of Materials;* 2014; 26; pp 5860-5867

Rousche, P. J.; R. A. Norman; 'Chronic intracortical microstimulation (ICMS) of cat sensory cortex using the Utah intracortical electrode array'; *IEEE Transactions on Rehabilitation Engineering*; 1999; 7; 1; pp 56-68

Sasaki, M.; B. C. Kaikkineth; K. Nagamine; H. Kaji; K. Torimitsu; M. Nishizawa; 'Highly conductive stretchable and biocompatible electrode-hydrogel hybrids for advanced tissue engineering'; *Ad. Healthcare Mater.*; 2014; 3; pp 1919-1927

Saracino, G. A. A.; D. Cigognini; D. Silva; A. Caprini; F. Gelain; 'Nanomaterials design and tests for neural tissue engineering'; *Chemical Society Reviews*; 2013; 42; pp 225-262

Sekine, S.; Y. Ido; T. Miyake; K. Nagamine; M. Nishizawa; 'Conducting polymer electrode printed on hydrogel'; *Journal of the American Chemical Society*; 2010; 132; pp 13174-13175

Sumrita, B.; A. Kumar; 'Biomaterials and bioengineering tomorrow's healthcare'; *Biomatter*; 2013; 3;3

Sun, J-Y.; X. Zhao; W. Illeperuma; O. Chauduri; K. H. Oh; D. Mooney; J. Vlassak; Z. Suo; 'Highy stretchable and tough hydrogels'; *Nature*; 2012; 489;133

Tessa, L.; B. Sood; M. Pecht; 'Field reliability estimation for cochlear implants'; *IEEE Transactions on Biomedical Engineering* (in press).

Tilley, Dana M.; RicardoVallejo; Courtney A. Kelley; Ramsin Benyamin; David L. Cedeno; 'A continuous spinal cord stimulation model attenuates pain-related behavior in vivo following induction of a peripheral nerve injury'; *Neuromodulation: Technologyat the Neural Interface*; 2014; DOI: 10.1111/ner.12280

Wang, L.; J. Shansky; C. Borselli; D. Mooney; H. Vanderburg; 'Design and fabrication of biodegradable, covalently cross linked shape-memory alginate scaffold for cell growth factor delivery'; *Tissue Engineering: Part A*; 2012; volume 18; number 19 and 20;

Williams, N. R.; M. S. Okun; 'Deep Brain Stimulation (DBS) at the interface of neurology and psychiatry'; *The Journal of Clinical Investigation*; 2013; volume 123; number 11; pp 4546-4556

Wilson, B. S.; M. F. Dorman; 'Cochlear implants: a remarkable past and a brilliant future'; *Hearing Research;* 2008; 242;0; pp 3-21

Wolter, T; 'Spinal cord stimulation for neuropathic pain: current perspective'; *Journal of Pain Research*; 2014; 7; pp651-663

World Health Organization; Neurological disorders public health challenges; 2007

Wu, Y.; B. Guo; P.X. Ma; 'Injectable electroactive hydrogels formed via host-guest interaction'; *ACS Macro Lett.*; 2014; 3; pp 1145-1150

Xiao, Y.; J. Che; 'An effective approach for fabrication of reinforced composite hydrogel engineered with single-walled carbon nanotubes (SWNTs), polypyrrole and PEGDA hydrogel'; *Journal of Material Chemistry*; 2012; 22; pp 8076-8082

Zhao, Y.; B. Liu; L. Pan; G. Yu; 'Three-dimensional (3D) nanostructure conductive polymer hydrogels for high-performance electrochemical devices'; *Energy & Environmental Sciences'*; 2013; 6; pp 2856-2870

Zeng, F. G.; S. Rebscher; W. V. Harrison; H. Feng; 'Cochlear implants: System design, Integration and Evaluation'; *IEEE Reviews in Biomedical Engineering*; 2008; 1; pp 115-142

Appendix A

Mechanical and electrical equations

This is the summary of mechanical, structural and electrical equations required for measuring mechanical, structural and electrical of gels.

A.1. Mechanical equations

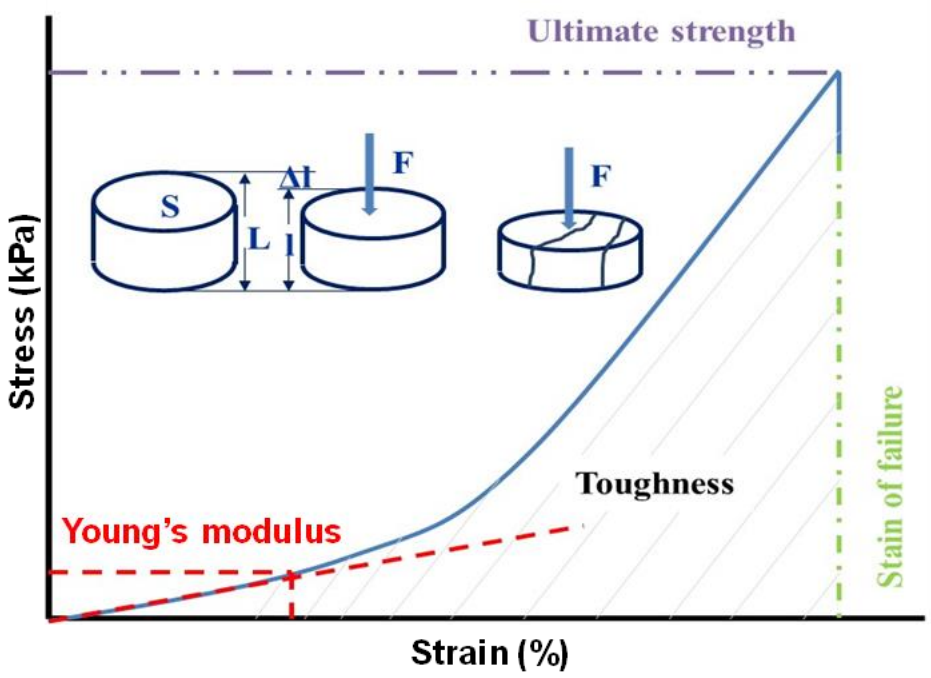

Figure A1. Several mechanical properties of a material can be quantitatively obtained from stress-strain curves. A. Schematic of how the mechanical properties are measured during gel compression up to gel failure. **B**. Example of stress-strain curve (dark blue) highlighting the modulus (diagonal red line), strain at failure (vertical dashed green line) and the ultimate strength (horizontal dashed purple line). The red dash lines are the examples of any arbitrary point at linear or elastic region which can be used to find the Young's modulus. S is surface area, L is initial height, Δl is dislocation, and F is applied force.

Stress: is the ratio of applied force (F) over gel's cross sectional area (S)

Eq.1 $$\sigma = \frac{F}{S}$$

Will be plotted vs strain, which is degree of deformation. The force unit in SI system is Newton (N). The surface area unit in SI system is square meter (m^2). Therefore, the stress unit in SI system is Newton per square meter (N/m^2) or Pascal (Pa). Engineering strain is a ratio of total deformation to the initial dimension.

Eq.2 $$\varepsilon = \frac{\Delta L}{L} = \frac{L-l}{L}$$

Which results in a dimensionless quantity.

The slope of the linear or elastic part of stress-strain curve is called Young's modulus or modulus of elasticity (fig. A1. the diagonal red line). It is the measure of gel's stiffness. It can be calculated by dividing the stress (fig. A1. the red horizontal dashed line) by the extensional strain (fig. A1. the red vertical dashed line) in the elastic/linear region of stress-strain curve:

Eq. 3 $$E = \frac{\sigma}{\varepsilon}$$

Due to the strain being dimensionless, Young's modulus has the same unit as stress which is Pascal (Pa).

Toughness is the ability of gels to absorbs energy and plastically deformed without fracturing. Toughness is the area under the stress-strain curve (fig. A1. the grey diagonal line).

Eq. 4 $$\frac{energy}{volume} = \int_0^{\varepsilon f} \sigma d\varepsilon$$

Toughness unit in SI system is J/m^3.

A.2 Pore interconnectivity Equations:

For pore interconnectivity, the mass of the sample will be measured with scale.

Eq.5 $$\%pore\ interconnectivity = \frac{Wb-Wa}{Wb}$$

Where:

Eq.6 $Wb = Wg + Wm + Wp$ (W_p are just the pours which are connected to the surface)

Eq.7 $$Wa = Wg + Wm$$

A.3 Electrical Equations:

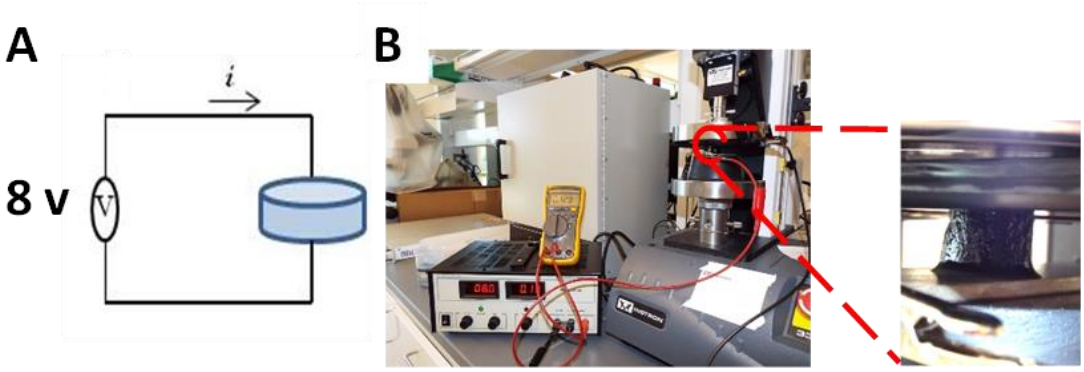

Figure A2. Electrical properties of each gel will be measured. A. Schematic of the electrical circuit used for recording the current. 8 volts is applied across a cylindrical gel (blue cylinder) and the current is measured. **B**. The set-up for recording the current under various strains with a zoomed-in image of a PEDOT cryogel under compression.

Samples are placed in the circuit similar to Figure A2. Different voltages (V) are applied, currents (I) are recorded and the resistances (R), resistivity (ρ) and electrical conductivity (σ) of the samples are calculated with ohm's law:

Eq.8 $$R = \frac{I}{V}$$

I is current and its unit is Amperes (A), V is voltage and its unit is volts (V) and resistance (R) unit is Ohms (Ω).

Eq. 9 $\rho = R\frac{S}{l}$

Where ρ is electrical resistivity, L is length (its unit is m) and S is surface area (its unit is m^2) and R is resistance (and its unit is Ω) and the resistivity unit is (Ω.m)

Eq. 10 $\sigma = \frac{1}{\rho}$

Where σ is electrical conductivity. The SI unit of conductivity is Siemens per meter (S/m).

Eq. 11 $G = \frac{I}{V}$

Where G is electrical conductance. The Si unit of conductance is Siemens (S)